The Journal *of* Immunology

RESEARCH ARTICLE | MARCH 01 2019

The B Cell Activation-Induced miR-183 Cluster Plays a Minimal Role in Canonical Primary Humoral Responses ⊘

Joseph N. Pucella; ... et. al

Related Content

miR-182 Is Largely Dispensable for Adaptive Immunity: Lack of Correlation between Expression and Function

J Immunol (March,2015)

In This Issue

J Immunol (March,2015)

The B Cell Activation-Induced miR-183 Cluster Plays a Minimal Role in Canonical Primary Humoral Responses

Joseph N. Pucella,* Montserrat Cols,* Wei-Feng Yen,* Shunbin Xu,[†] and Jayanta Chaudhuri*

Although primary humoral responses are vital to durable immunity, fine-tuning is critical to preventing catastrophes such as autoimmunity, chronic inflammation, and lymphomagenesis. MicroRNA (miRNA)-mediated regulation is particularly well suited for fine-tuning roles in physiology. Expression of clustered paralogous miR-182, miR-96, and miR-183 (collectively, 183c) is robustly induced upon B cell activation, entry into the germinal center, and plasmablast differentiation. $183c^{GT/GT}$ mice lacking 183c miRNA expression exhibit largely normal primary humoral responses, encompassing class switch recombination, affinity maturation, and germinal center reaction, as well as plasmablast differentiation. Our rigorous analysis included ex vivo class switch recombination and plasmablast differentiation models as well as in vivo immunization with thymus-dependent and thymus-independent Ags. Our work sways the debate concerning the role of miR-182 in plasmablast differentiation, strongly suggesting that 183c miRNAs are dispensable. In the process, we present a valuable framework for systematic evaluation of primary humoral responses. Finally, our work bolsters the notion of robustness in miRNA:target interaction networks and advocates a paradigm shift in miRNA studies. *The Journal of Immunology*, 2019, 202: 1383–1396.

P athogen-specific neutralizing Abs are a key weapon deployed by adaptive immune defense systems safeguarding jawed vertebrates against infection. The B cell lineage is the driving force of humoral responses that are necessary for Ab-mediated protection (1). Despite their value, humoral responses must be tightly regulated for several reasons. For one, aberrant Ab activity is often at the center of autoimmune pathologic conditions, for example in systemic lupus erythematosus, in which autoantibodies specific for nucleic acid direct host tissue damage (2, 3). Another impetus for meticulous regulation hinges on the intense proliferative bursts and genomic instability that are typical of humoral responses. An example is during the germinal center (GC) response wherein Ag-specific GC B cells are coerced into rounds of clonal proliferation and intentional DNA damage for Ig secondary diversification processes (4). Lymphomagenic transformation of B cells is an inherent hazard accompanying humoral responses, evidenced by the correlation of persistent GCs, and inflammation in general, with cancer (5, 6). Thus, a nuanced understanding of the mechanisms regulating humoral response quality and magnitude is a vital goal, with immediate translatable implications in modulating vaccine potency as well.

Of particular interest is the DNA mutator activation-induced deaminase (AID), specifically expressed in activated B cells and necessary to promote Ab diversity via Ig class switch recombination (CSR) and somatic hypermutation (SHM) (7–9). We were initially drawn to the conundrum faced by activated B cells in balancing DNA damage repair responses: subtly subverting faithful repair to allow efficient CSR and SHM while simultaneously averting catastrophic genome instability and chromosomal translocation is a delicate undertaking. The requisite fine-tuning for such a precarious balance prompted our interest in microRNAs (miRNAs).

miRNAs comprise a class of short, ~21-nt RNA that employ RNA-silencing complexes containing Argonaute proteins to achieve regulation of gene expression via mRNA transcript degradation and/or translational inhibition (10, 11). In the brief time since their discovery, there has been an explosion of interest in miRNA-mediated mechanisms of regulation; well-accepted roles for miRNAs seemingly pervade all disciplines, including embryonic development, immunology, and oncology (12–18). Because of the authority of the short, ~6-nt seed sequence in directing target interactions and the relatively nonstringent criteria the seed sequence imposes, it is not uncommon for a single miRNA species to bind and repress hundreds of transcripts, typically via target sites located in transcript 3′ untranslated regions. For each individual target, repression need not be absolute but may in fact be quite modest. Consequently, miRNA-mediated regulation is capable of subtle manipulation of entire gene networks, a desirable feature for the precise fine-tuning expected to be necessary during humoral responses (19, 20). Taken together with the fact that repression via translational inhibition is rapid and reversible, miRNA-mediated regulation of humoral responses is an intriguing prospect.

*Immunology Program, Memorial Sloan Kettering Cancer Center, Gerstner Sloan Kettering Graduate School, New York, NY 10065; and †Department of Ophthalmology, Visual and Anatomical Sciences, Wayne State University School of Medicine, Detroit, MI 48201

ORCIDs: 0000-0001-5711-2626 (W.-F.Y.); 0000-0002-6140-0943 (S.X.); 0000-0002-3838-0075 (J.C.).

Address correspondence and reprint requests to Dr. Jayanta Chaudhuri, Mortimer B. Zuckerman Research Center, Memorial Sloan Kettering Cancer Center, 417 East 68th Street, New York, NY 10065. E-mail address: chaudhuj@mskcc.org

The online version of this article contains supplemental material.

Abbreviations used in this article: aCI, anti-CD40 plus IL-4; aCII, anti-CD40 plus IL-4 plus IL-5; AID, activation-induced deaminase; 183c, miR-183 cluster; CSR, class switch recombination; DZ, dark zone; FDC, follicular dendritic cell; GC, germinal center; IF, immunofluorescence; LI, LPS plus IL-4; LII, LPS plus IL-2 plus IL-5; LN, lymph node; LTD, LPS plus TGF-β plus anti–IgD-dextran; LZ, light zone; miRNA, microRNA; qPCR, quantitative PCR; SHM, somatic hypermutation; SRBC, sheep RBC; TD, thymus-dependent; Tfh, follicular Th cell; TI, thymus-independent; WT, wild-type.

Previously, we reported robust, AID-dependent induction of miR-182 upon activation of mature naive B cells undergoing CSR. Despite this suggestive expression pattern, as well as published roles in the DNA damage response (21, 22) and clonal activation of CD4^{+} Th cells (23), we showed that mice with a genetic deletion of the *Mir182* locus (*Mir182*^{−/−}) manifested no significant defect in the development of the adaptive immune system, the capacity of B cells to undergo CSR, or the GC response to a model Ag. We also found miR-182 to be dispensable in both CD4^{+} and CD8^{+} T cells during ex vivo activation and *Listeria monocytogenes* infection, including secretion of Th1 effector cytokines (24). The puzzling discordance between miR-182 expression and observed phenotype elicited the notion of compensatory mechanisms masking the effect of miR-182 elimination. Subsequently, we hypothesized the existence of compensation by miR-96 and miR-183, two highly related family members of miR-182. Perhaps miR-183 and miR-96 alone can meet the biological threshold for necessary repression of miR-182 targets in the context of activated B cells, thus compensating for miR-182 absence.

In this work, we have comprehensively characterized the effect of abrogating expression of the entire miR-183 cluster (183c), constituted by paralogous family members miR-183, miR-96, and miR-182, on canonical B cell–centric primary humoral responses. In particular, we investigated CSR, the GC response, and extrafollicular plasmablast differentiation. Much to our surprise, we find yet again the absence of a significant phenotype, despite vigorous induction of expression. We conclude that, if there is a compensatory mechanism upon loss of miR-182 in B cells, it is not solely mediated by clustered family members. Hence, this work not only highlights miRNA network redundancy but in doing so offers a practical blueprint for methodical, rigorous analysis of primary humoral immune responses.

Materials and Methods

Mice

The generation of 183c[GT/GT] and *Mir182*^{−/−} mice has been described (25, 26). For all experiments, we strived to use 6–10-wk-old healthy mice of both genders, with sex-matched littermate wild-type (WT) controls. When littermate controls were unavailable, care was taken to use closely age- and sex-matched mice from different litters. Mouse colonies were maintained according to Institutional Animal Care and Use Committee policies.

Purified B cell cultures

Naive mature B cells were purified by negative selection from RBC-lysed splenocyte cell suspensions using MACS anti-mouse CD43 microbeads (no. 130-049-801; Miltenyi Biotec) on a MidiMACS magnetic separation apparatus (Miltenyi Biotec). Purified cells were cultured in B cell media (sterile-filtered RPMI 1640 [no. 22400-089; Life Technologies] plus 15% FBS [no. 35-010-CV; Corning] plus 1% additional ʟ-glutamine [200 mM stock] plus 1% penicillin/streptomycin mixture [no. 400-109; Gemini] plus 0.0005% 2-ME [no. BP176-100; Fisher Scientific]) and stimulated with various conditions: LPS (20 μg/ml, no. L4130; Sigma-Aldrich), LI (LPS [20 μg/ml] plus IL-4 [12.5 ng/ml, no. 404-ML-010; R&D Systems]), LII (LPS [20 μg/ml] plus IL-2 [100 U/ml, recombinant human; National Institutes of Health] plus IL-5 [5 ng/ml, no. 215-15; PeproTech]), LTD (LPS [10 μg/ml] plus TGF-β [2 ng/ml, no. 240-B-010; R&D Systems] plus anti–IgD-dextran [0.33 μg/ml, FinaBio no. 0001; Fina Biosolutions]), aCI (anti-CD40 [0.5 μg/ml, clone HM40-3, no. 16-0402-86; eBioscience] plus IL-4 [12.5 ng/ml]), and aCII (anti-CD40 [0.5 μg/ml] plus IL-4 [12.5 ng/ml] plus IL-5 [2 ng/ml]). Cell cultures were initiated at 0.5×10^6 cells/ml and split 1:2 at 48 and 72 h. Flow cytometric analysis of CFSE staining was performed according to the manufacturer's instructions (CellTrace CFSE Cell Proliferation Kit Protocol; Invitrogen).

Real-time quantitative PCR

All RNA was prepared from cell samples using standard TRIzol (no. 15596026; Invitrogen/Thermo Fisher Scientific) protocol. All quantitative PCR (qPCR) experiments were performed in 384-well format on an Applied Biosystems QuantStudio 6 Flex instrument. miRNA qPCRs were done using the following components from Applied Biosystems (Thermo

Fisher Scientific): TaqMan miRNA Reverse Transcription Kit (no. 4366596), TaqMan Universal Master Mix II, no UNG (no. 4427788), TaqMan miRNA Assays (no. 4427975: miR-182 ID 002599, miR-96 ID 000186, miR-183 ID 00269, snoRNA251 ID 001236). miRNA data were normalized to snoRNA251 transcript level. mRNA qPCRs were done using the following components from Thermo Fisher Scientific: Invitrogen SuperScript IV VILO Master Mix (no. 11756050), Applied Biosystems TaqMan Fast Advanced qPCR Master Mix (no. 4444557), Applied Biosystems TaqMan Gene Expression Assays (no. 4448892: *CcnD2* ID Mm00438071_m1, *FoxO1* ID Mm00490672_m1, *Bach2* ID Mm00464379_m1, *Adcy6* Mm00475773_g1, *Dock4* ID Mm00555659_m1, *Ago2* ID Mm00838341_m1, *Ywhaz* ID Mm01158417_g1). mRNA data were normalized to *Ywhaz* transcript level. Data analysis was performed using the comparative Ct method (27).

Intracellular flow cytometry staining

To stain for Blimp1, Bcl6, and Ki67, cells were fixed and permeabilized using BioLegend True-Nuclear Transcription Factor Buffer Set (no. 424401). To stain for intracellular Ig, cells were fixed and permeabilized using BD Biosciences CytoFix/CytoPerm Fixation/Permeabilization Solution Kit (no. 554715), omitting the GolgiStop step.

Sheep RBC immunization

Packed 100% sheep RBCs (SRBCs) were purchased from Innovative Research (no. IC100-0210). Mice were immunized i.p. with 1×10^9 SRBCs in sterile PBS per 200-μl dose on day 0, boosted on day 10, and sacrificed on day 14.

NP-CGG immunization

NP(31)-CGG (no. N-5055D-5; Biosearch Technologies) was precipitated with Imject alum adjuvant (no. 77161; Thermo Fisher Scientific). Mice were immunized i.p. in 200-μl doses with 50 or 100 μg on day 0 and boosted with 50 μg on day 10 (as indicated in legends for Figs. 4 and 5). Mice were sacrificed on day 14, or serum was collected by standard submandibular bleeding procedure on days 0, 7, 21, and 28 (as indicated in figure legend).

Immunofluorescence

Spleen samples from immunized mice were embedded in optimal cutting tissue reagent (Sakura). Tissue sections of 6–10 μm thickness were stained with primary Abs, followed by appropriate secondary reagents. Primary Abs with irrelevant binding activity and the appropriate secondary reagents were used to validate the specificity of tissue staining. Coverslips were applied with FluorSave (Calbiochem). Slides were scanned with Panoramic Flash (3DHistech) using 20×/0.8NA objective, and regions of interest were drawn manually using CaseViewer (3DHistech) and exported into TIFF files. Raw unedited images were then analyzed using ImageJ/FIJI, by which the area of the interest (B cell GC) was automatically measured. In all cases, DAPI channel of the scan was used as a mask to exclude artifacts outside the tissue. For all images, scoring of desired area was done manually with randomly shuffled pictures to reduce any bias.

ELISA

Assays were done in Thermo Fisher Scientific MaxiSorp clear, flat-bottom, 96-well plates (no. 439454). Coating Abs for binding IgM, IgG1, IgG2b, IgG2c, IgG3, and IgA were purchased from SouthernBiotech (no. 1020-01, 1070-01, 1090-01, 1079-01, 1100-01, and 1040-01, respectively). The following isotype standards were used to calculate absolute concentration values: IgM (no. 14-4752-81; eBioscience), IgG1 (no. 0102-01; SouthernBiotech), IgG2b (no. 14-4732-81; eBioscience), IgG2c (no. 0122-01; SouthernBiotech), IgG3 (no. 553486; BD Pharmingen), and IgA (no. 553478; BD Pharmingen). Secondary Abs for detecting IgM, IgG1, IgG2b, IgG2c, IgG3, and IgA were purchased from SouthernBiotech (no. 1020-05, 1070-05, 1090-05, 1079-05, 1100-05, and 1040-05, respectively). eBioscience ELISA diluent (no. 00-4202-56) was used as blocking buffer, eBioscience TMB substrate (no. 00-4201-56) was used to develop, and 1 M phosphoric acid was used to stop development. Plates were read at 450 nm on a BioTek Synergy HT detector. Absolute concentrations of serum Abs were determined by interpolation from the standard curve, with attention paid to keeping within standard and sample linear ranges. All samples were done in duplicate over a four-step dilution series. An eight-step standard curve was generated for each plate. For NP-specific assays, plates were coated with NP(4)-BSA (no. N-5050L-10; Biosearch Technologies) or NP(>20)-BSA (no. N-5050H-10; Biosearch Technologies). Relative titers were determined by interpolation on the plate reference curve generated for each plate using a constant sample, with attention paid to keeping within plate reference and sample linear ranges. All samples were done in duplicate over an eight-step dilution series.

Jh4 intron SHM analysis

GC B cells (B220$^+$ CD38$^-$ IgD$^-$ CD138$^-$ GL7$^+$ PNA$^+$) were FACS-sorted from Peyer patches. Genomic DNA was isolated and amplified by PCR using Phusion High-Fidelity DNA Polymerase (no. M0530S; New England Biolabs) according to the manufacturer's instructions and the following primers: 5′-GGA ATT CGC CTG ACA TCT GAG GAC TCT GC-3′ (forward) and 5′-GAC TAG TCC TCT CCA GTT TCG GCT GAA TCC-3′ (reverse). The PCR products were gel-purified and cloned into Zero Blunt TOPO (no. K280020; Invitrogen). Individual transformed bacterial colonies were sent to GeneWiz for Sanger sequencing using the following primer: 5′-CCA TAC ACA TAC TTC TGT GTT CC-3′. Sequence analysis was performed using SeqMan Pro (DNASTAR).

LPS immunization

TLR*grade* LPS from *Salmonella minnesota* R595 (no. ALX-581-008-L002) was purchased from Enzo Life Sciences. Mice were immunized i.v. with 50 μg in sterile PBS per 200-μl dose on day 0 and sacrificed on day 3.

NP-Ficoll immunization

NP(30)-AECM-Ficoll (NP-Ficoll; no. F-1420-10) was purchased from Biosearch Technologies. Mice were immunized i.p. with 100 μg in sterile PBS per 200-μl dose on day 0 and sacrificed on day 5.

ELISpot

Assays were done in Millipore Multi-Screen HA filtration 96-well plates (no. MSIPN4W). IgM, IgG1, and IgG3 coating Abs were the same as for ELISA. Secondary Abs were purchased from Vector Laboratories for detecting IgM (no. BA-2020) and IgG (no. BA-9200), followed by HRP-Avidin D (no. A-2004; Vector Laboratories). For NP-specific assays, plates were coated with NP(>20)-BSA (no. N-5050H-10; Biosearch Technologies). PBS plus 2% BSA was used as blocking buffer, ELISpot AEC substrate
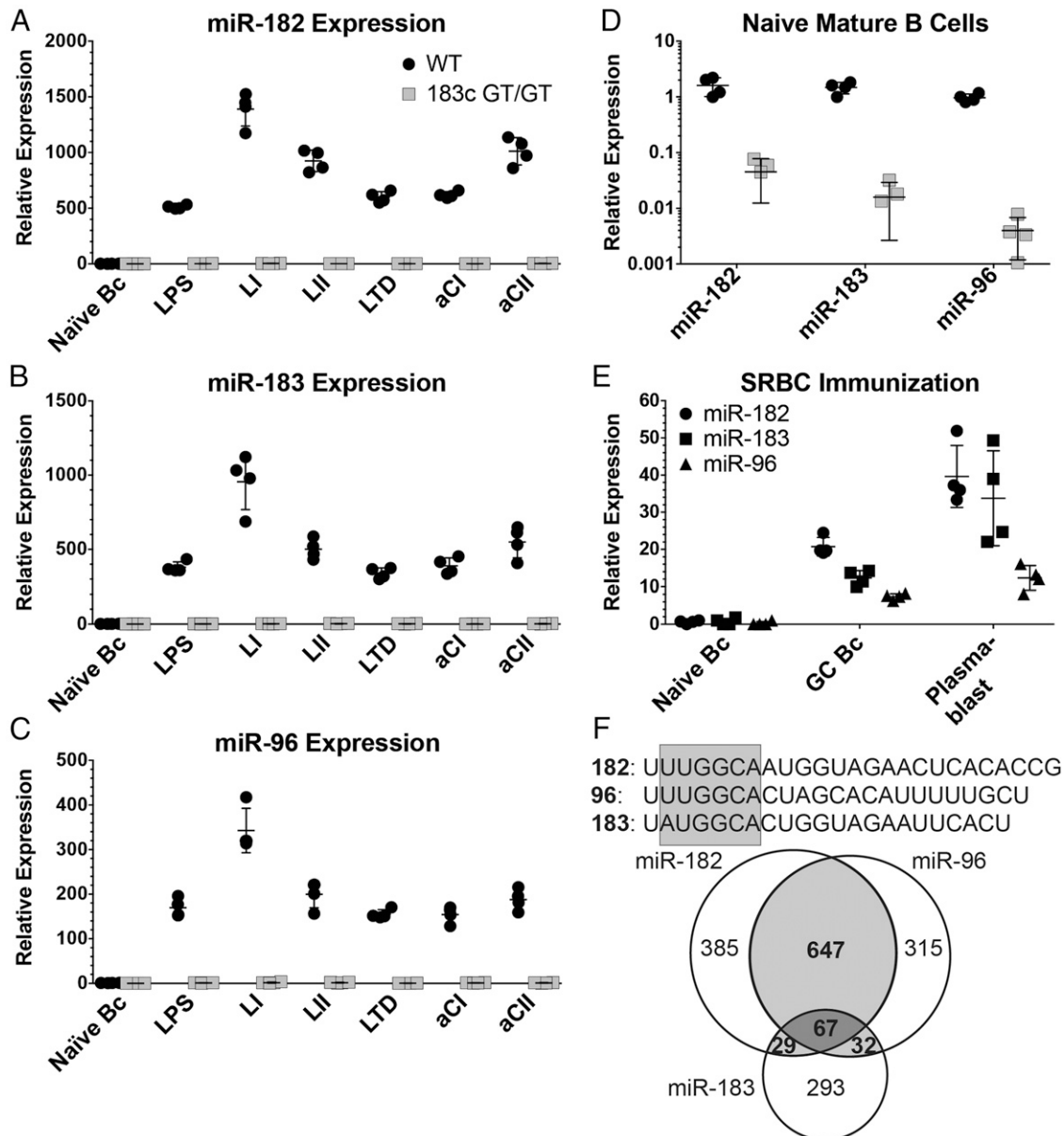

FIGURE 1. 183c expression is induced upon B cell activation. (**A–D**) Expression level of miR-182 (A), miR-183 (B), and miR-96 (C) in MACS-sorted murine splenic mature B cells ex vivo stimulated for 96 h, determined by real-time qPCR. $n = 4$, one experiment. (D) 183c expression in murine splenic naive B cells. $n = 4$, one experiment. (**E**) 183c expression level in splenic naive B cells (B220$^+$ CD38$^+$ IgD$^+$ CD138$^-$ GL7$^-$ PNA$^-$), GC B cells (B220$^+$ CD38$^-$ IgD$^-$ CD138$^-$ GL7$^+$ PNA$^+$), and plasmablasts (B220^{lo} CD138$^+$ GL7$^-$ PNA$^-$) FACS-sorted from SRBC-immunized WT mice. $n = 4$, one experiment. (**F**) Sequences of 183c miRNAs and diagram of TargetScan predicted target overlap. Gray box over sequence alignment indicates seed region. Circle area is to scale with predicted target number. See Supplemental Table II for full list of predicted targets. Statistical significance was determined by unpaired *t* test. All WT versus 183c$^{GT/GT}$ and naive versus activated differences were deemed highly significant; see Supplemental Table I for *p* values.

(no. 551951; BD Biosciences) was used to develop. Plates were scanned on a CTL ImmunoSpot S6 Entry instrument and analyzed using CTL ImmunoSpot software, version 7.0.9.5. All samples were done over a 12-step dilution series. Plotted spots per 10^6 cells were determined by averaging spots per 10^6 cells over a minimum of three different dilutions, with attention paid to using wells within the linear range. Counting parameters were held constant across all plates of the same assay type. Quality control of automated counting was performed on every plate by visual inspection.

Bone marrow harvest

Bone marrow was flushed out of femurs with B cell media and treated with ACK buffer to lyse RBCs.

Flow cytometry

All samples were acquired with an LSR II flow cytometer (Becton Dickinson) and data were analyzed with FlowJo software (Tree Star).

Statistical analysis

The p values were determined by ratio paired t test or two-tailed unpaired t test, as indicated. The ratio paired t test was preferred in most cases to manage difficulties in obtaining homogeneous experimental cohorts. A value $\alpha = 0.05$ was used in all experiments. All error bars represent SD.

Results

183c miRNAs are highly expressed in activated B cells, GC B cells, and plasmablasts

miR-182, -96, and -183 (here, collectively referred to as 183c) are clustered in an intronic locus on murine chromosome 6 and may be synchronously expressed as part of a polycistronic transcript (25). Given that miR-182 is so strongly induced upon B cell activation, yet its absence is of debatable consequence (24, 28), we sought to carefully investigate the expression of the entire 183c family. As expected (24, 28), vigorous mature miR-182 induction was observed by qPCR in mature B cells stimulated ex vivo (Fig. 1A). Interestingly, the expression patterns of mature miR-183 (Fig. 1B) and miR-96 (Fig. 1C) in B cells activated by the same assortment of stimuli closely mirror that of miR-182, albeit with less pronounced induction.

This suggests that, in B cells, transcription and processing of these genomically clustered miRNAs are linked. Our observations are concordant with published reports indicating miR-182 is induced by IL-2 in Th cells via STAT5 (23) and by IL-4 in regulatory T cells via cMaf (29). miR-183 has also been shown to be induced in human NK cells by TGF-β (30); however, TGF-β inhibited 183c miRNA expression in mouse Th17 cells (31), so the relationship appears to be context-dependent. Similarly, a parallel pattern was observed for 183c miRNA expression in GC B cells and plasmablasts induced upon immunization with SRBCs (Fig. 1E).

Because of their expression pattern, overwhelming sequence homology, and predicted target overlap as determined using the TargetScan 7.1 algorithm (Fig. 1F) (32), we reasoned that miR-183 and miR-96 might provide sufficient redundancy to miR-182 to mask the individual loss of miR-182. To investigate the role of 183c miRNAs in B cell function, we employed the 183c$^{GT/GT}$ mouse model in which a gene trap construct inserted upstream of 183c abrogates expression of all 183c miRNAs (25, 33). We confirmed that 183c miRNA expression was abolished in B cells and plasmablasts derived from 183c$^{GT/GT}$ mice (Fig. 1). The 183c$^{GT/GT}$ mouse model thus provided a convenient model to assess the requirements of 183c miRNAs in B cell development and function. We also selected six mRNA candidates predicted to be targeted by every 183c member. We found no significant changes in expression between WT and 183c$^{GT/GT}$ naive and GC B cells or in plasmablasts (Supplemental Fig. 1). This may indicate that these genes are not true targets of 183c in this context or may hint at additional layers of compensation at play.

183c$^{GT/GT}$ mice exhibit normal B cell development and peripheral B cell populations

We first characterized B cell development and homeostasis in 183c$^{GT/GT}$ mice. In bone marrow, we observed frequencies of pro (CD43$^+$ B220^{lo} IgM$^-$), pre (CD43$^-$ B220^{lo} IgM$^-$), immature (B220^{lo} IgM$^+$), and mature recirculating (B220^{hi} IgM$^+$) B cells indistinguishable from WT (Supplemental Fig. 2A). In the periphery, we
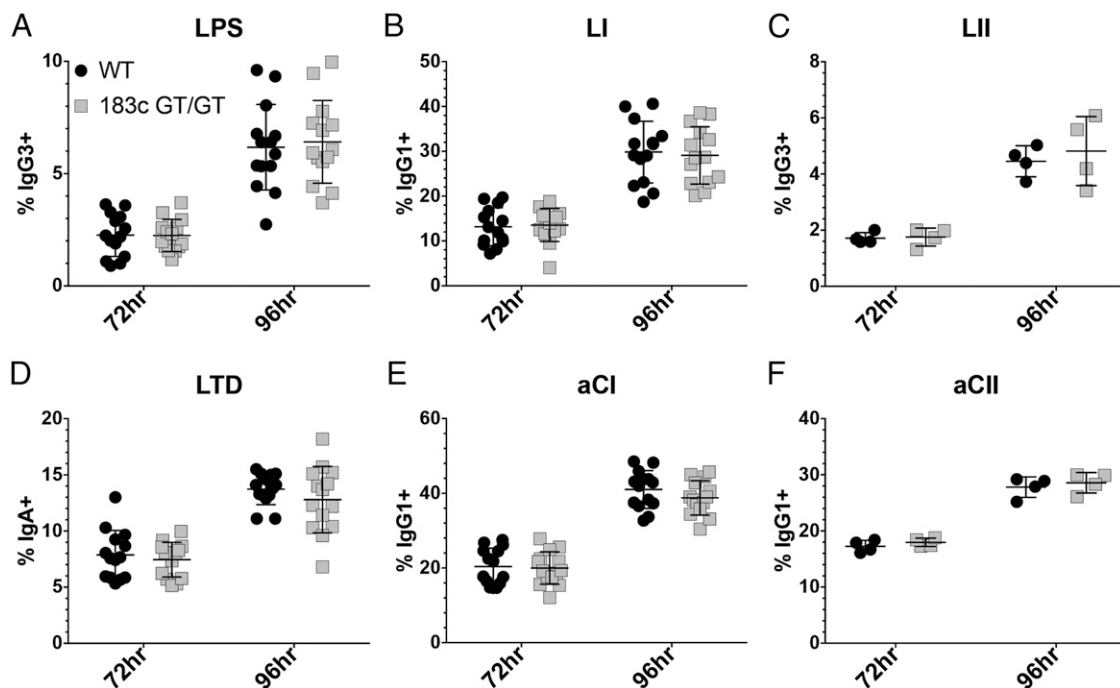
FIGURE 2. 183c is dispensable for CSR in B cells stimulated ex vivo. (**A–F**) MACS-sorted murine splenic mature B cells were cultured and monitored by flow cytometry at 72 and 96 h for frequency of surface IgG3$^+$ cells upon LPS (A) and LII (C) stimulation; IgG1$^+$ upon LI (B), aCI (E), and aCII (F) stimulation; and IgA$^+$ upon LTD stimulation (D). $n = 14$ for LPS, LI, LTD, and aCI (five experiments); $n = 4$ for LII and aCII (one experiment). Statistical significance was determined by ratio paired t test. All WT versus 183c$^{GT/GT}$ comparisons failed to meet statistical significance ($\alpha = 0.05$).
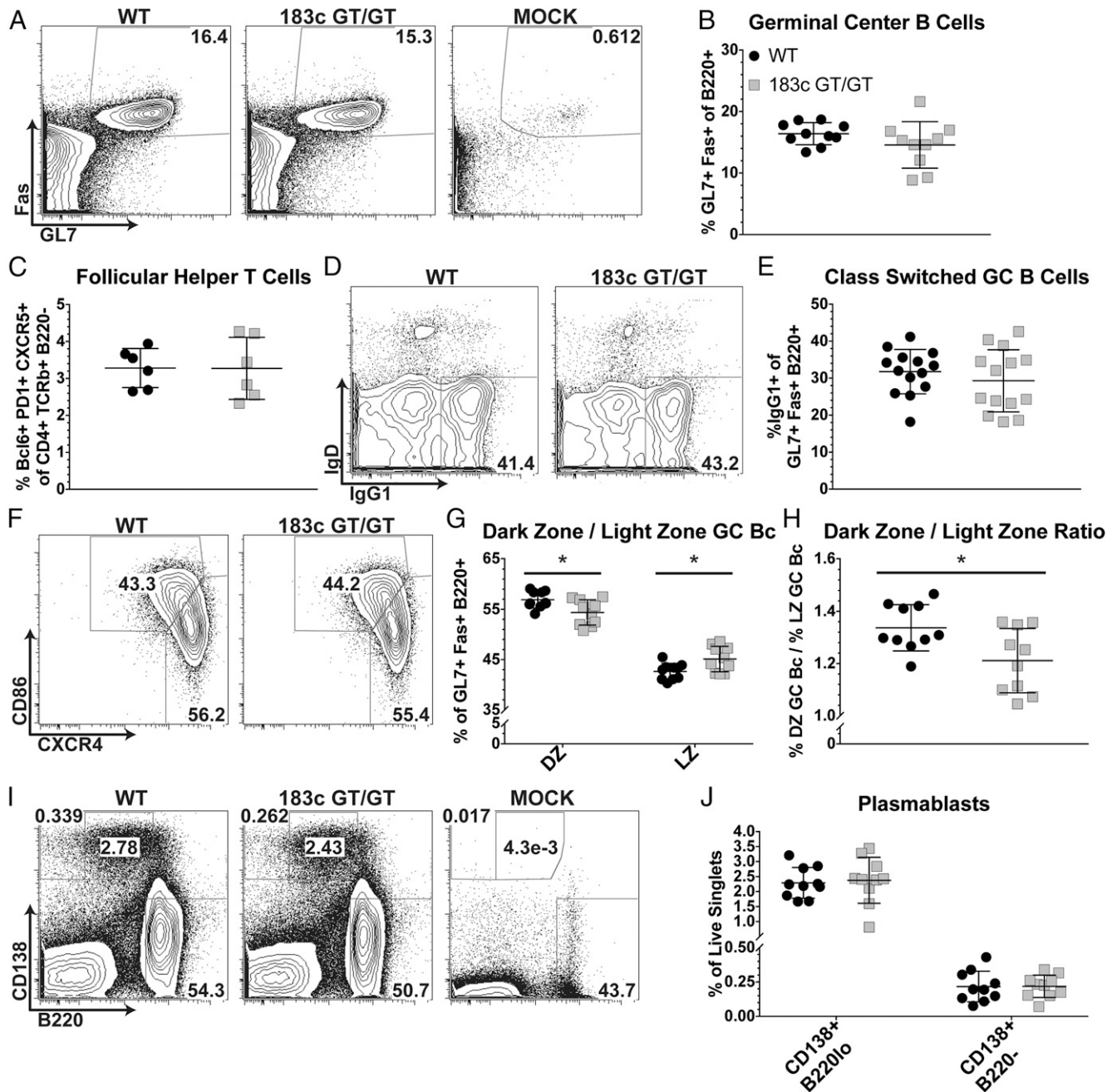
FIGURE 3. SRBC-immunized 183c$^{GT/GT}$ mice exhibit normal, although LZ skewed, GCs. 183c$^{GT/GT}$ and WT littermates were immunized i.p. with 1×10^9 SRBCs, boosted on day 10, and sacrificed on day 14. Total splenocytes were analyzed by flow cytometry. (**A** and **B**) Representative flow cytometry plots (A) and quantification (B) of GC B cell frequency (GL7$^+$ Fas$^+$ B220$^+$). (**C**) Quantification of Tfh frequency (Bcl6$^+$ PD1$^+$ CXCR5$^+$ of CD4$^+$ TCRβ$^+$ B220$^-$). $n = 4$, one experiment. (**D** and **E**) Representative flow cytometry plots (D) and quantification (E) of isotype-switched IgG1$^+$ GC B cell frequency (IgG1$^+$ of GL7$^+$ Fas$^+$ B220$^+$). (**F–H**) Representative flow cytometry plots (F), quantification of DZ (CXCR4^{hi} CD86^{lo}) and LZ (CXCR4^{lo} CD86^{hi}) GC B cell frequency (of GL7$^+$ Fas$^+$ B220$^+$) (G), and DZ/LZ ratio (H). (**I** and **J**) Representative flow cytometry plots (I) and quantification (J) of plasmablast (CD138$^+$ B220^{lo}) and plasmacyte (CD138$^+$ B220$^-$) frequency. All $n = 10$, two experiments, except (H). Statistical significance determined by ratio paired t test. *$p < 0.05$.

observed similar spleen cellularity (Supplemental Fig. 2B) and frequency of splenic follicular (IgM^{int} IgD$^+$ CD21$^+$ CD23$^+$) and marginal zone (IgM$^+$ IgD$^-$ CD21^{hi} CD23^{lo}) B cells (Supplemental Fig. 2C). Judging by surface IgM and IgD expression, we ascertained peripheral staging of B cell maturity in the spleen to be normal (Supplemental Fig. 2C). In total, B cell development appears to be unimpaired by ubiquitous loss of 183c miRNA expression.

CSR is unperturbed by 183c miRNA ablation

We first identified miR-182 as a promising candidate for regulating CSR in activated B cells in part because of robust induction upon

activation by CSR-stimulating conditions and a significant dependency on AID sufficiency for this induction. Ultimately, we reported no CSR defect in *Mir182$^{-/-}$* B cells (24). In continuation of this work and to investigate possible compensation within the 183c cluster, we first sought to test if purified B cells from 183c$^{GT/GT}$ mice could efficiently undergo CSR in ex vivo culture. To our surprise, we found no difference in the ability of 183c$^{GT/GT}$ to undergo CSR compared with WT, regardless of stimulation protocol (Fig. 2A–F). We conclude that expression of 183c miRNAs is not cell-intrinsically necessary for CSR and that the lack of a CSR phenotype in *Mir182$^{-/-}$* B cells was not due to compensation by miR-183 or miR-96.
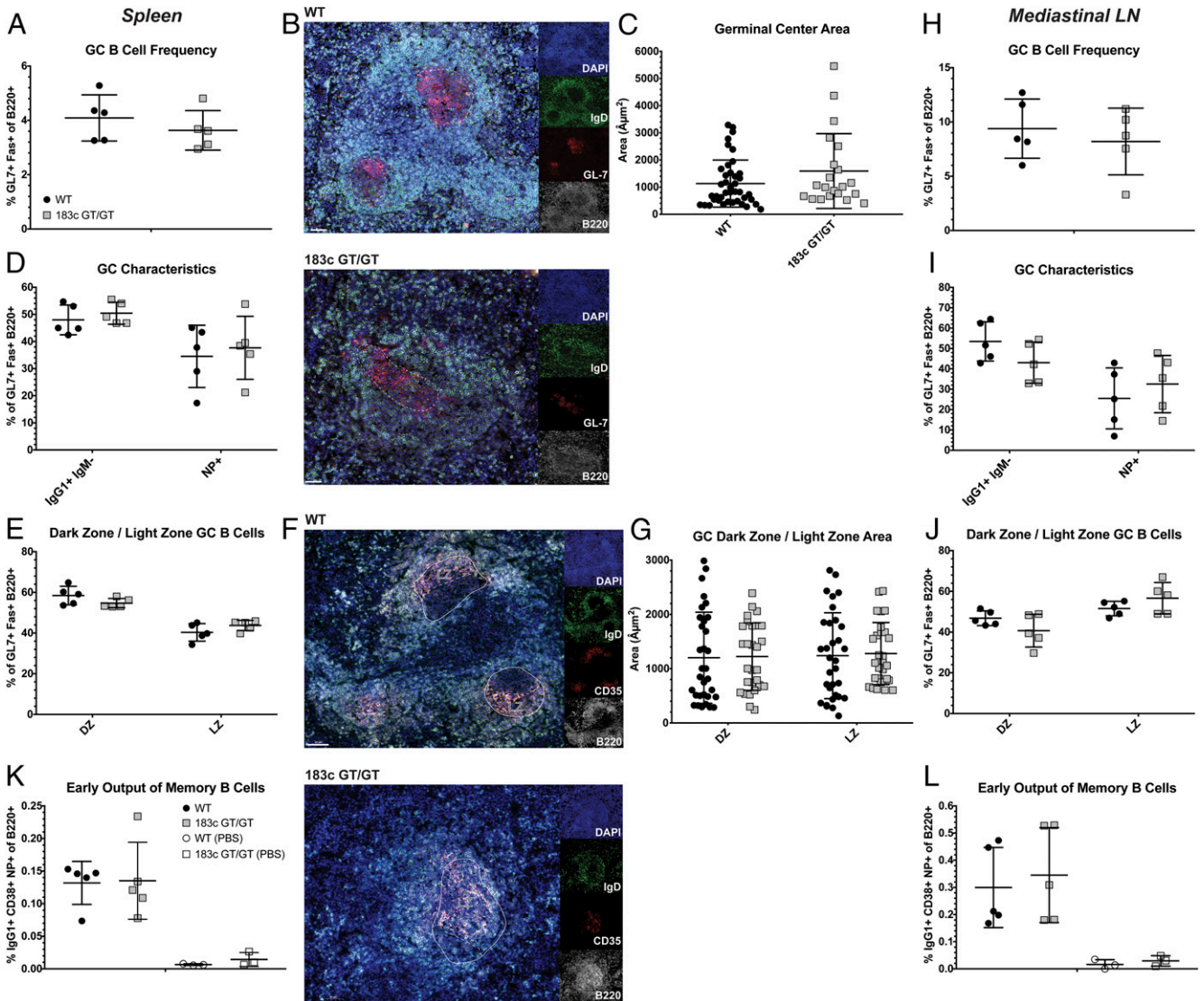
FIGURE 4. 183c$^{GT/GT}$ mice immunized with TD Ag NP-CGG exhibit normal GCs. 183c$^{GT/GT}$ and WT littermates were i.p. immunized with 100 μg of NP(31)-CGG in alum, boosted on day 10, and sacrificed on day 14. Total splenocytes (**A**, **D**, **E**, and **K**) and mediastinal LN cells (**H**, **I**, **J**, and **L**) were analyzed by flow cytometry. Spleen sections were analyzed by IF imaging; scale bar, 50 μm (**B**, **C**, **F**, and **G**). (A and H) Quantification of GC B cell frequency (GL7$^+$ Fas$^+$ of B220$^+$). (B and C) Representative images (B) and quantification (C) of GC area (GL7$^+$ IgD$^-$ B220$^+$). (D and I) Quantification of isotype-switched IgG1$^+$ (IgG1$^+$ IgM$^+$ of GL7$^+$ Fas$^+$ B220$^+$) and Ag-specific (NP$^+$ of GL7$^+$ Fas$^+$ B220$^+$) GC B cell frequency. (E and J) Quantification of DZ (CXCR4^{hi} CD86^{lo}) and LZ (CXCR4^{lo} CD86^{hi}) GC B cell frequency (of GL7$^+$ Fas$^+$ B220$^+$). (F and G) Representative images (F) and quantification (G) of GC LZ area (CD35$^+$ IgD$^-$ B220$^+$). (K and L) Quantification of isotype-switched, Ag-specific early memory B cell frequency (IgG1$^+$ CD38$^+$ NP$^+$ of B220$^+$). $n = 5$, one experiment. Statistical significance was determined by ratio paired t test. All WT versus 183c$^{GT/GT}$ comparisons failed to meet statistical significance ($\alpha = 0.05$).

During a humoral response, B cells are potentially exposed to complex arrays of stimuli including Ag, TLR ligands, secreted cytokines (e.g., IL-4, IL-21, BAFF), and membrane-bound CD154, the ligand for B cell-expressed CD40 canonically provided by follicular Th cells (Tfh) (34–37). Ex vivo stimulatory conditions mimic physiology in principle, but supraphysiological delivery of signaling molecules neglects intricate nuances of signaling cross-talk and cellular interactions known to occur in vivo. To overcome these caveats, we turned to thymus-dependent (TD) and -independent (TI) Ag in vivo immunization model systems.

GCs in 183c$^{GT/GT}$ mice are normal with only a modest light-zone skew

SRBC immunization is a complex polyepitope TD Ag model system that induces robust GC reactions, whereby CSR and affinity maturation occur (38–40). In response to SRBC immunization, we observed strong induction of GL7$^+$ Fas$^+$ GC B cells. There was a slight trend for reduced GC B cell frequency in 183c$^{GT/GT}$, but the disparity was not statistically significant (Fig. 3A, 3B).

In spleens from unimmunized mice, we found a substantial reduction in total T cell frequency, accompanied by a propensity for increased frequency of CD8$^+$ T cells at the expense of CD4$^+$ T cells (Supplemental Fig. 2E). This was surprising because it was not upheld in lymph node (LN) samples (Supplemental Fig. 2F), and thymic TCRβ$^+$ cells were actually somewhat elevated in 183c$^{GT/GT}$ mice (Supplemental Fig. 2D), suggesting there is no block in early T cell development. Because CD4$^+$ Tfh cells are necessary for initiating and sustaining GC reactions (41), we were concerned by the observed reduction in homeostatic splenic CD4$^+$ T cells, because this is the population from which Tfh cells derive. Thus, we quantified the frequency of Tfh cells upon SRBC immunization as the percentage of CD4$^+$ TCRβ$^+$ B220$^-$ cells that
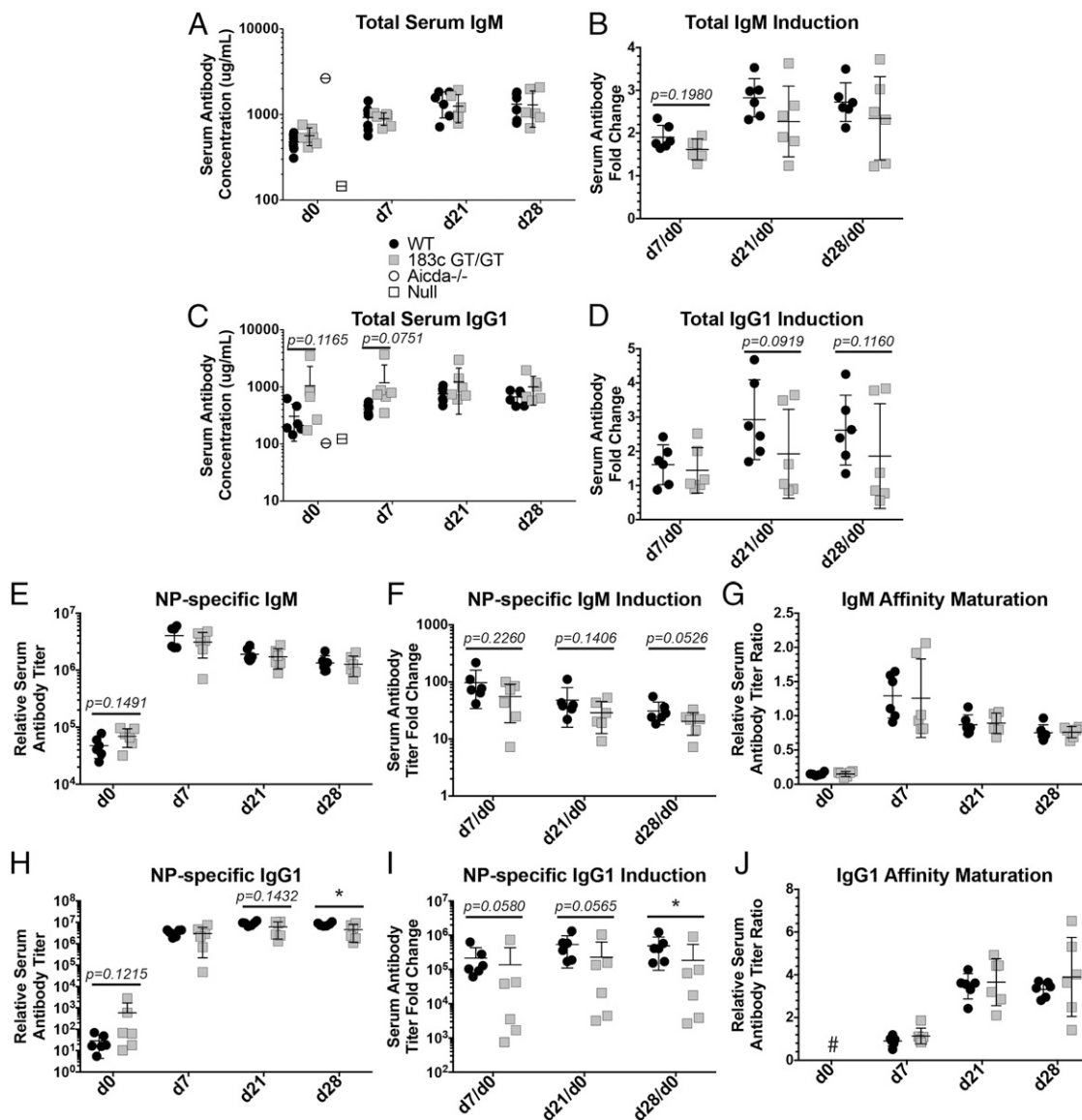
FIGURE 5. $183c^{GT/GT}$ mice immunized with TD Ag NP-CGG trend for reduced serum Ab induction, although affinity maturation remains intact. (**A–J**) $183c^{GT/GT}$ and WT littermates were immunized with 100 μg of NP(31)-CGG in alum, and serum was collected on days 0, 7, 14, 21, and 28. ELISA-based quantification of serum total IgM concentration (A) and induction (B), total IgG1 concentration (C) and induction (D), NP-specific IgM titer (E) and induction (F), and NP-specific IgG1 titer (H) and induction (I). $Aicda^{-/-}$ and null (empty well) are shown to demonstrate isotype specificity and assay limit of quantification, respectively (A and C). Affinity maturation was assessed by ratio of high affinity (NP4) to broad (NP20) Ag binding for IgM (G) and IgG1 (J). IgG1 affinity maturation was indeterminate (#) at day 0, as NP(4)-BSA–binding IgG1 levels were below the level of quantification (J). $n = 6$, one experiment. Statistical significance was determined by ratio paired t test. *$p < 0.05$.

were Bcl6$^+$ PD1$^+$ CXCR5$^+$. We observed normal Tfh frequency in $183c^{GT/GT}$ mice (Fig. 3C), suggesting that GC reactions also appear normal from the T cell perspective.

B cells activated during SRBC immunization undergo CSR predominantly to IgG1 (39). Thus, we interrogated the frequency of surface IgG1$^+$ B cells within GCs as a readout of capacity to undergo CSR in vivo. As expected, we observed prolific CSR, with roughly 30% of WT GC B cells being IgG1$^+$. The mean of $183c^{GT/GT}$ samples was minimally decreased relative to WT, but the difference was not statistically significant (Fig. 3D, 3E).

The GC is a microanatomical structure that can be spatially divided into a dark zone (DZ) and light zone (LZ), through which GC B cells cycle. The DZ, constituted chiefly by GC B cells marked by high CXCR4 and low CD86 surface expression, is characterized by intense B cell proliferation and AID-mediated SHM of loci

encoding Ig H and L chains. In contrast, the LZ is comprised of CD86^{hi} CXCR4^{lo} GC B cells, follicular dendritic cells (FDCs), and Tfh cells that dictate selection of B cells with enhanced binding to Ag, thus driving affinity maturation (34). Accordingly, we assessed the balance of DZ to LZ GC B cells as an indicator of GC condition. We found that SRBC-induced $183c^{GT/GT}$ GCs were slightly but statistically significantly LZ skewed (Fig. 3F–H).

To further characterize the GC response in $183c^{GT/GT}$ mice, we used NP-CGG immunization, a well-characterized hapten TD Ag model system that facilitates identification of Ag (NP)-specific GC B cells and secreted Abs (42, 43). In agreement with the results observed with SRBC immunization, the frequency of splenic GC B cells was similar between WT and $183c^{GT/GT}$ mice upon NP-CGG immunization (Fig. 4A). This was corroborated by immunofluorescence (IF) imaging of B220$^+$ IgD$^-$ GL7$^+$ splenic GCs
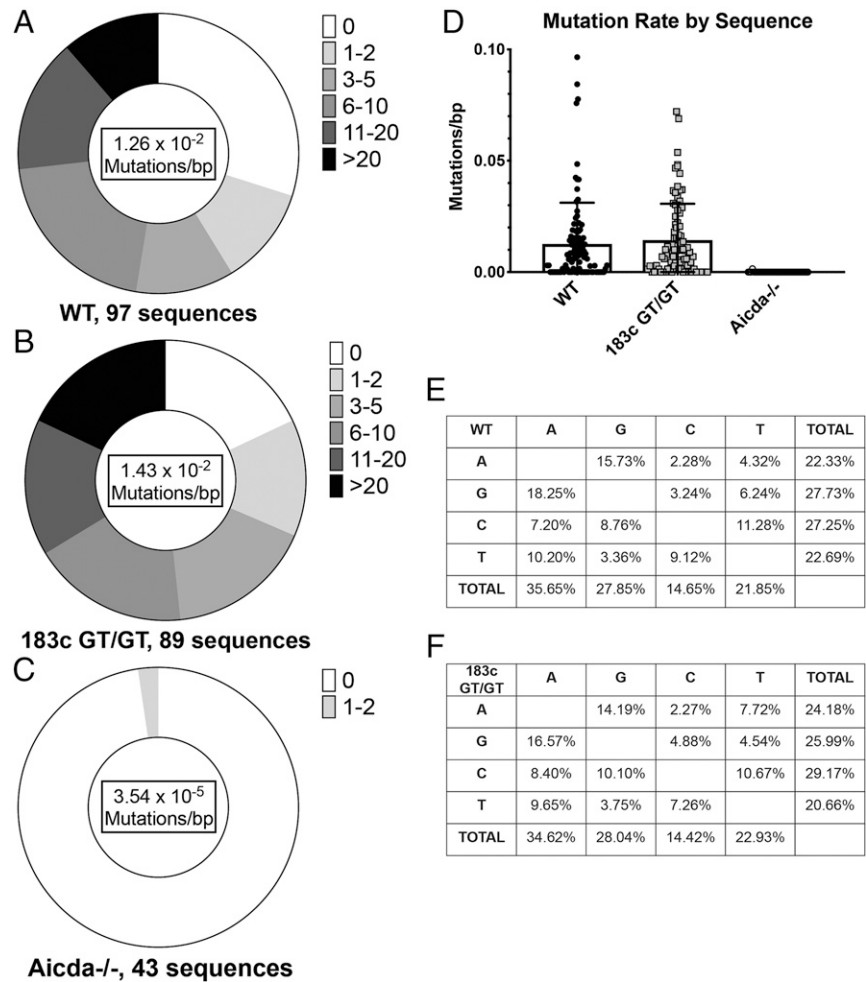
FIGURE 6. Somatic hypermutation is unaffected by 183c loss. GC B cells (B220^{+} CD38^{−} IgD^{−} CD138^{−} GL7^{+} PNA^{+}) were FACS-sorted from Peyer patches of 183c[GT/GT] and WT littermates. DNA was isolated, individual *IgH* Jh4 introns were cloned, and clones were Sanger sequenced. DNA from *Aicda*^{−/−} GC B cells was used to assess baseline mutation detection. (**A–C**) Number of mutations per sequence and mutation rates per bp were calculated for WT (A), 183c[GT/GT] (B), and *Aicda*^{−/−} (C) genotypes. (**D**) Mutation rates per sequence were calculated. Statistical significance was determined by ratio paired *t* test. The WT versus 183c[GT/GT] comparison failed to meet statistical significance ($\alpha = 0.05$). (**E** and **F**) The mutation spectrum was broken down by reference (columns) and mutated nucleotide (rows) for WT (E) and 183c[GT/GT] (F). *n* = 3, one experiment.

E

WT	A	G	C	T	TOTAL
A		15.73%	2.28%	4.32%	22.33%
G	18.25%		3.24%	6.24%	27.73%
C	7.20%	8.76%		11.28%	27.25%
T	10.20%	3.36%	9.12%		22.69%
TOTAL	35.65%	27.85%	14.65%	21.85%	

F

183c GT/GT	A	G	C	T	TOTAL
A		14.19%	2.27%	7.72%	24.18%
G	16.57%		4.88%	4.54%	25.99%
C	8.40%	10.10%		10.67%	29.17%
T	9.65%	3.75%	7.26%		20.66%
TOTAL	34.62%	28.04%	14.42%	22.93%	

(Fig. 4B, 4C). The frequency of class-switched IgG1 positivity and NP specificity was also unchanged among GC B cells (Fig. 4D). Surprisingly, the LZ skew observed in SRBC-induced GCs was less apparent in NP-CGG–induced GCs. Assessed by flow cytometry, there was a slight trend (Fig. 4E). However, no difference was discernible by IF imaging of splenic GC DZs (CD35^{−}) and LZs (CD35^{+}) (Fig. 4F, 4G).

Finally, we looked at NP-CGG–induced GCs in mediastinal LNs, a site for which Ag delivery will differ substantially from splenic follicles. Consistent with the splenic data, we found no significant differences in total, IgG1^{+}, NP[+], DZ, and LZ B cell frequencies, although there was again a trend for LZ skew in 183c[GT/GT] GCs (Fig. 4H–J). In sum, we conclude that 183c[GT/GT] GCs appear essentially normal, although exhibiting a mild LZ skew at times.

Early memory B cell output is unaffected by loss of 183c miRNAs

It is conceivable that the timing of 183c miRNA induction in the GC is such to play a role in the cell fate decision upon GC exit (i.e., toward memory or plasma fate). To evaluate this possibility, we observed the emergence of Ag-specific memory B cells in both spleen and mediastinal LN upon NP-CGG immunization. Because of the phenotypic similarity of naive and memory B cells, we quantified only IgG1^{+} switched cells to add confidence to our analysis. We found no difference in early memory B cell (IgG1^{+} CD38^{+} NP^{+} B220^{+}) frequency between WT and 183c[GT/GT] mice (Fig. 4K, 4L). We conclude that 183c miRNAs do not play a major role in memory B cell formation in this context.

183c[GT/GT] mice manifest a trend for reduced induction of serum Abs, although affinity maturation remains intact

To delve deeper, we harvested serum from NP-CGG–immunized mice and quantified serum Abs by ELISA. We found no statistically significant differences at days 0, 7, 21 and 28 postimmunization in the serum concentration of total IgM (Fig. 5A) and IgG1 (Fig. 5A). We did observe a consistent trend across all time points observed for reduced induction of serum IgM and IgG1 relative to day 0; however, the differences were not statistically significant (Fig. 5B, 5D). Next, we evaluated serum titer of NP-specific IgM and IgG1 Abs. Here we witnessed an analogous pattern to the total isotype assays: few differences at individual time points (only NP-specific IgG1 at day 28 was significantly different) (Fig. 5E, 5H) but simultaneously a consistent downward trend in fold change induction rates (Fig. 5F, 5I). It should be noted that the consistent trend for reduced serum Ab induction in 183c[GT/GT] mice might be driven by the trend for slightly elevated serum Ab in 183c[GT/GT] at day 0 seen in all assays. In line with this interpretation, no apparent defect in 183c[GT/GT] plasmablast differentiation after SRBC immunization was noted (Fig. 3I, 3J).

Importantly, although there may be a minor effect on induction of serum Ab, affinity maturation is distinctly unperturbed by the loss of 183c miRNAs as evidenced by equivalent ratios of high affinity (NP4) to broad affinity (NP20) binding between WT and 183c[GT/GT] IgM (Fig. 5G) and IgG1 (Fig. 5J) serum Abs. To further probe affinity maturation, we directly measured selection-independent SHM rates by sequencing the *IgH* Jh4 introns from Peyer's patch GC B cells. This region, which flanks the 3′-border
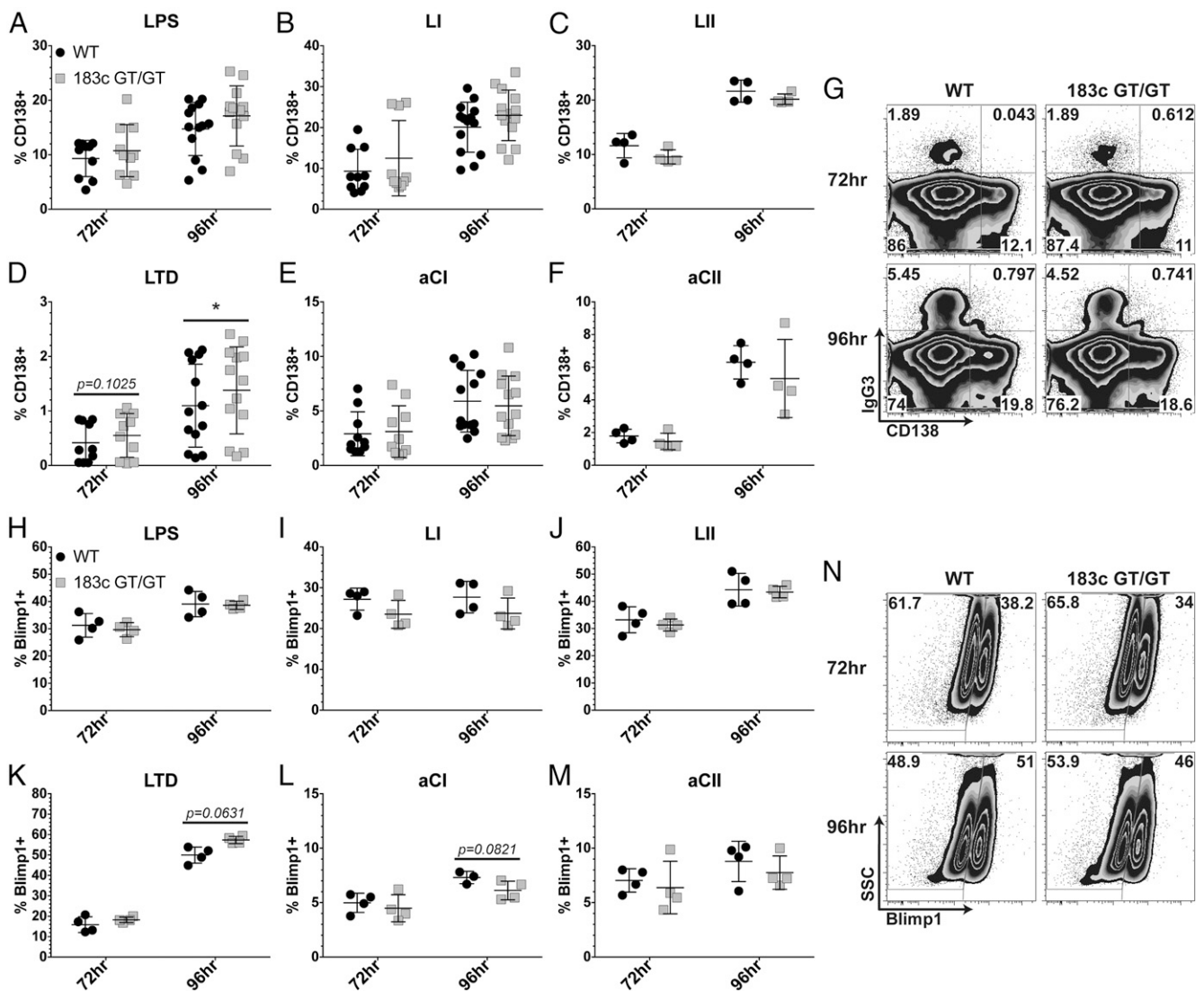
FIGURE 7. Ex vivo plasmablast marker induction is normal in absence of 183c expression. MACS-sorted murine splenic mature B cells were cultured and monitored by flow cytometry at 72 and 96 h. (**A–F**) Frequency of $CD138^+$ cells upon LPS (A), LI (B), LII (C), LTD (D), aCI (E), and aCII (F) stimulation. $n = 14$ for 96 h LI (five experiments); $n = 13$ for 96 h LPS, LTD, and aCI (four experiments); $n = 10$ for 72 h LPS, LI, LTD, and aCI (three experiments); $n = 4$ for LII and aCII (one experiment). (**G**) Representative flow cytometry plots of LPS-stimulated B cells. (**H–M**) Frequency of intracellular $Blimp1^+$ cells upon LPS (H), LI (I), LII (J), LTD (K), aCI (L), and aCII (M) stimulation. $n = 4$, one experiment. (**N**) Representative flow cytometry plots of LII-stimulated B cells. Statistical significance was determined by ratio paired t test. *$p < 0.05$.

of all rearranged V gene segments, is generally found to be heavily mutated in GC B cells in response to food Ags and is regarded as a bona fide measure of SHM (44). We found comparable rates of mutation between WT and $183c^{GT/GT}$ genotypes (Fig. 6A–D). In addition, we found no significant differences in the spectrum of mutations observed (Fig. 6E, 6F). GC B cells from $Aicda^{-/-}$ mice were analyzed as control (Fig. 6C). These results assert that 183c miRNAs are not important for Ab affinity maturation.

In conclusion, these results hint at a potential role for 183c miRNAs in promoting plasmablast differentiation and/or plasmablast function (e.g., the secretion of Abs per se). NP-CGG immunization induces both extrafollicular (45) and post-GC plasmablast differentiation (46). Given that we observed starker differences in NP-specific Ab induction at later time points (Fig. 5E, 5F, 5H, 5I), these results lend more support to an effect of 183c miRNAs in plasmablasts of post-GC, rather than extrafollicular, origin. Interestingly, a defective extrafollicular response in $Mir182^{-/-}$ mice immunized with NP-CGG and, separately, NP-Ficoll was recently

demonstrated using ELISA and ELISpot. The significant reduction observed in the titer of NP-specific IgG1 serum Ab and frequency of NP-specific IgG1-secreting plasmablasts at early time points postimmunization led Li et al. (28) to conclude that miR-182 plays a prominent role in promoting extrafollicular plasmablast differentiation. The role of 183c miRNAs in plasmablasts evidently requires further elucidation to resolve these inconsistencies. On a separate note, the lack of perceived impact on affinity maturation, assessed by NP-specific ELISA and direct measurement of SHM rates, reinforces the claim that GC reactions are functional overall in $183c^{GT/GT}$ mice.

Induction of plasmablast markers and soluble Ab in culture does not require 183c expression

In light of the discordance among our results and published data (28), we initially turned back to our ex vivo culture system to interrogate the role of 183c miRNAs in the plasma fate decision. One benefit of this approach is that the arsenal of conditions at our disposal can be employed to fuel various degrees of Ab secretion

FIGURE 8. Ab secretion in cultured B cells is not significantly impaired by 183c miRNA ablation. MACS-sorted murine splenic mature B cells were cultured, and supernatant was harvested at 96 h for ELISA. (A–E) Concentration of IgM (A), IgG1 (B), IgG3 (C), IgG2b (D), and IgA (E) in culture supernatant upon indicated stimulation protocol. $n = 4$, one experiment. Statistical significance was determined by ratio paired t test. $*p < 0.05$, $***p < 0.0005$.
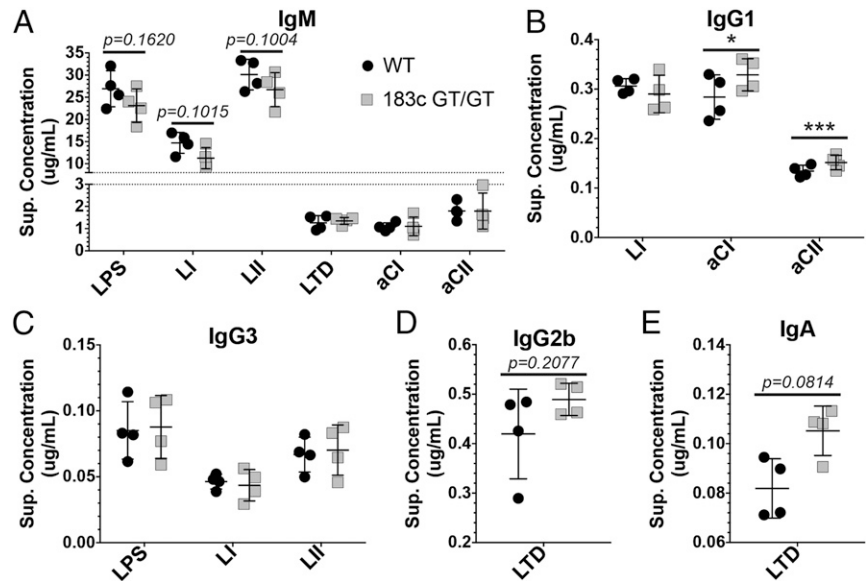
and induction of characteristic plasmablast markers such as CD138 and Blimp1, the master transcriptional regulator of the plasma lineage (47). Likewise, simultaneous use of protocols impinging on different signaling pathways may offer a broad perspective on the plasmablast fate decision and specific contexts in which 183c miRNAs may be involved. We again used six different protocols to stimulate purified naive mature splenic B cells, as described for Figs. 1 and 2. Strikingly, we found no significant defect in expression of plasmablast markers CD138 (Fig. 7A–G) and intracellular Blimp1 (Fig. 7H–N), in 183c$^{GT/GT}$ cultured B cells across all stimulation protocols. In fact, we uncovered a statistically significant increase in CD138$^+$ cells upon LTD stimulation at both 72 and 96 h. Although not statistically significant, it is noteworthy that Blimp1$^+$ cell frequency upon LTD stimulation trends in the same way. Overall, it is unmistakable that these ex vivo B cell culture results reveal no defect in the efficiency of 183c$^{GT/GT}$ B cells to induce expression of plasmablast markers.

From the same cultures, we harvested supernatant samples to measure soluble Ab concentration by ELISA. We found a trend for reduced IgM levels from 183c$^{GT/GT}$ B cells cultured with LPS, LI, and LII stimulation (Fig. 8A), although the trend did not achieve statistical significance and was not echoed in LTD-, aCI-, and aCII-stimulated cultures (Fig. 8A). Notably, we also did not see this trend when measuring other isotypes, instead finding statistically significant increases in supernatant IgG1 levels from 183c$^{GT/GT}$ B cell cultures upon aCI and aCII stimulation (Fig. 8B), no difference in IgG3 levels, irrespective of stimulation method (Fig. 8C), and trends for increases in both IgG2b (Fig. 8D) and IgA (Fig. 8E) levels upon LTD stimulation. On the whole, our data are not consistent with a defect in Ab secretion per se. The trend for context-dependent reduced soluble IgM but not other isotypes may warrant further investigation.

Humoral responses to both TI-1 and TI-2 Ags do not depend on 183c miRNA expression

To extend our findings beyond ex vivo stimulation, we once again employed in vivo immunization models, this time with TI Ags that are dominated by the extrafollicular humoral response and plasmablast differentiation (48–50). When immunizing with these TI Ags, GC B cells were undetectable above background, as expected (data not shown).

First, we measured the extrafollicular response to i.v. immunization with TI-1 Ag LPS by quantifying CD138$^+$ B220^{lo} plasmablasts

using flow cytometry (51). We observed an equivalent proportion in WT and 183c$^{GT/GT}$ mice (Fig. 9A, 9B). Similarly, we found no difference in the appearance of Blimp1$^+$ cells, nor any disparity in the frequency of Blimp1 positivity in various CD138$^+$ subsets (Fig. 9C, 9D). As anticipated, an overwhelming majority of CD138$^+$ plasmablasts have not undergone CSR and exhibit readily detectable high levels of intracellular IgM, indicating that they likely secrete Ab (Fig. 9E, 9F). No difference was noted between WT and 183c$^{GT/GT}$ except a slight decrease in the frequency of intra-IgM$^+$ among CD138$^+$ B220$^-$ plasmacytes (Fig. 9F). Overall, we conclude that, upon systemic LPS administration, 183c miRNAs are not necessary to mount an extrafollicular response composed of rapid and robust plasmablast differentiation.

Finally, we immunized mice with the TI-2 Ag NP-Ficoll and performed ELISpot to measure the frequency of total and Ag-specific plasmablasts in the spleen (52, 53). Similar to TI-1 Ag, we did not detect a significant difference between WT and 183c$^{GT/GT}$ samples in the frequency of IgM (Fig. 10A), IgG1 (Fig. 10B), IgG3 (Fig. 10C), NP-specific IgM (Fig. 10D, 10E), and NP-specific IgG (Fig. 10F, 10G) Ab-secreting cells. We tested *Mir182$^{-/-}$* mice to contextualize what we observe in 183c$^{GT/GT}$ mice, but quite unexpectedly, we also detected no defect in *Mir182$^{-/-}$* mice (Fig. 10A–D, 10F). It is noteworthy that we detected very little difference between mock- and NP-Ficoll–immunized animals in frequency of total IgM, IgG1, and IgG3 Ab-secreting cells (Fig. 10A–C), whereas the difference was stark for NP-specific assays (Fig. 10D–G). This highlights the subtlety and specificity of this immunization protocol in producing Ag-specific plasmablasts. In summary, we conclude that expression of 183c miRNAs is nonessential for TI Ag–driven plasmablast differentiation. Further experimentation will be required to delineate if 183c miRNAs fulfill a particular role during humoral responses that is uniquely accessed during experimental immunization with the simple hapten TD Ag NP-CGG, yet not with the more complex, polyepitope TD Ag SRBC or with TI-1 Ag LPS and TI-2 Ag NP-Ficoll.

Overall, our results do not support the published role for miR-182 in plasmablast differentiation (28), especially the aforementioned results in *Mir182$^{-/-}$* mice immunized with NP-Ficoll (Fig. 10). A potential explanation for this inconsistency is alluded to by the discordance in frequency of NP-specific IgG1-secreting plasmablasts present at day 5 in WT mice. Whereas we quantified a mean of nearly 200 secreting
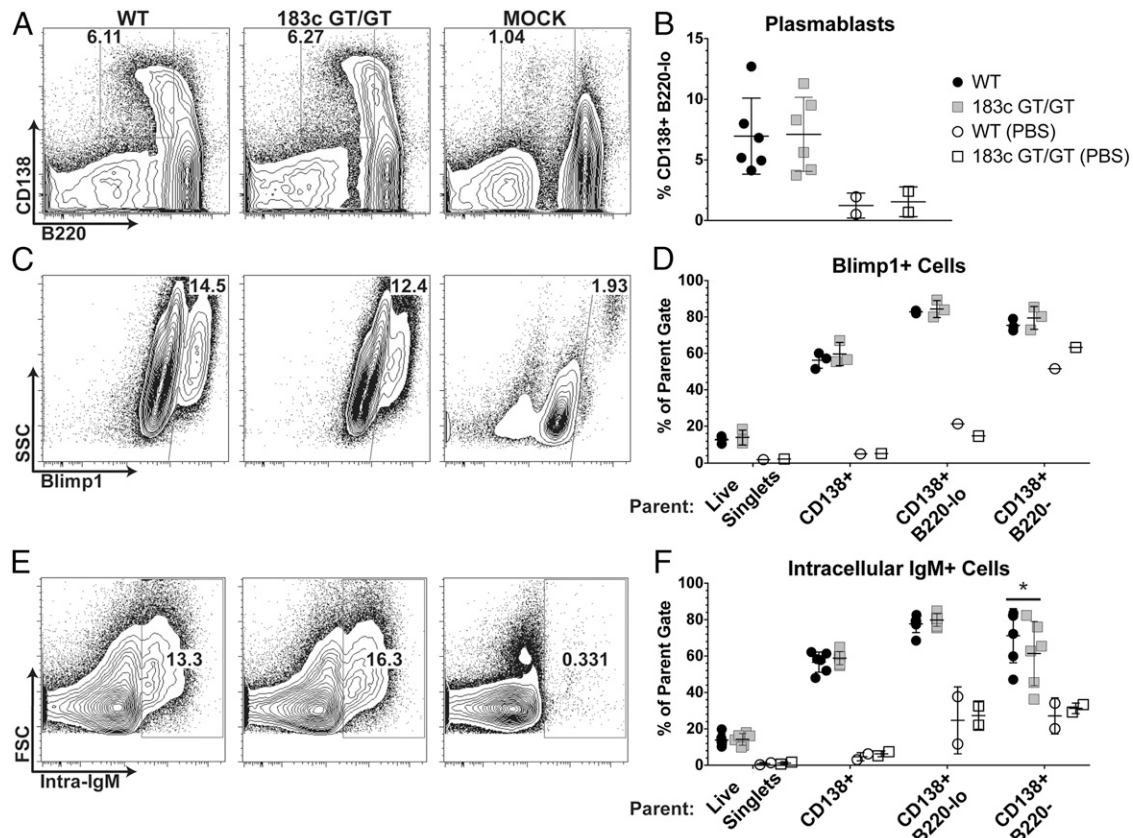
FIGURE 9. 183c miRNAs are not required for humoral response to TI-1 Ag LPS. 183c$^{GT/GT}$ and WT littermates were i.v. immunized with 50 µg of LPS in sterile PBS and sacrificed on day 3. Total splenocytes were analyzed by flow cytometry. Representative flow cytometry plots (**A**) and quantification (**B**) of plasmablast (CD138$^+$ B220^{lo}) frequency. All $n = 6$, except $n = 2$ for mock immunization (PBS) controls; two experiments. Representative flow cytometry plots (**C**) and quantification (**D**) of intracellular Blimp1$^+$ cell frequency. All $n = 3$, except $n = 1$ for mock PBS controls; one experiment. Representative flow cytometry plots (**E**) and quantification (**F**) of intracellular IgM$^+$ frequency. All $n = 6$, except $n = 2$ for mock immunization (PBS) controls; two experiments. Statistical significance was determined by ratio paired t test. *$p < 0.05$.

cells per million splenocytes, only ~20 were enumerated in the published study (28). The disagreement of our results with even WT samples may hint at disparate immunization potency or assay sensitivity, potentially illuminating why our results diverge. Nonetheless, the multitude of approaches we have employed, both ex vivo and in vivo, give us confidence in the assertion that 183c miRNAs play at best a minor role in extrafollicular plasmablast programs.

Discussion

In this work, we have provided compelling evidence that 183c miRNAs, although dramatically induced, play a minor role in mature B cell functions including CSR, the GC reaction, and, in contrast to previous results, extrafollicular plasmablast response (28). We have laid out a comprehensive framework for interrogating proximal events occurring during canonical humoral responses.

Our results convincingly argue against a role for 183c miRNAs in the emergent phenomena of the GC reaction and affinity maturation during the response to TD Ags. Successful affinity maturation relies on the coordination of activities among GC B cells, Tfh cells, stromal populations (e.g., FDCs), and myeloid cells (e.g., subcapsular sinus and tingible-body macrophages). The lack of an effect on GCs in 183c$^{GT/GT}$ mice suggests little to no impact of 183c miRNAs on SHM and the ability of GC B cells to process and present Ag. Because of the ubiquitous lack of 183c expression in these mice, our results also suggest the dispensability of 183c miRNAs for the capacity of Tfh to bestow selection-guiding survival signals to GC B cells upon MHC class II–mediated Ag

presentation and of FDCs to support B cell maintenance and distribute Ag to GC B cells, as the GC reaction inevitably collapses without these B cell–extrinsic functions (34).

Unexpectedly, despite the lack of any major effect on GC responses, SRBC-induced 183c$^{GT/GT}$ GCs display significantly altered DZ to LZ GC B cell balance. One possible explanation is that 183c$^{GT/GT}$ GC B cells have reduced proliferative capacity while in the DZ state, in which the majority of GC B cell proliferation occurs (34, 54). However, GC B cell frequency remained largely unaltered, and Ki67 expression was comparable between WT and 183c$^{GT/GT}$ GCs (Supplemental Fig. 2G). Likewise, CSR efficiency was normal both in vivo and ex vivo even though CSR is inexorably dependent on proliferation (55–57). Additionally, there was no observed defect in ex vivo proliferative capacity, as the CFSE dilution rate was in fact trending higher in 183c$^{GT/GT}$ B cells (Supplemental Fig. 2H). Another explanation for the LZ tilt of 183c$^{GT/GT}$ GCs is that 183c miRNA-mediated target repression governs the passage of GC B cells through LZ/DZ transient cell states, reinforcing DZ and/or promoting departure from LZ phenotype. In this regard, *FoxO1*, a transcription factor implicated in programming the DZ state (58, 59), has been demonstrated to be a miR-182 target in other cell types (23, 31, 60). However, if miR-182 were to repress *FoxO1* in GC B cells, one would expect 183c$^{GT/GT}$ GCs to instead be DZ skewed. In addition, *FoxO1* disruption in GC B cells would have caused a drastic deficiency in CSR and reduced SHM (58, 59). Finally, we measured the levels of *FoxO1* transcript in WT and 183c$^{GT/GT}$ GC B cells and found no significant difference (Supplemental Fig. 1).
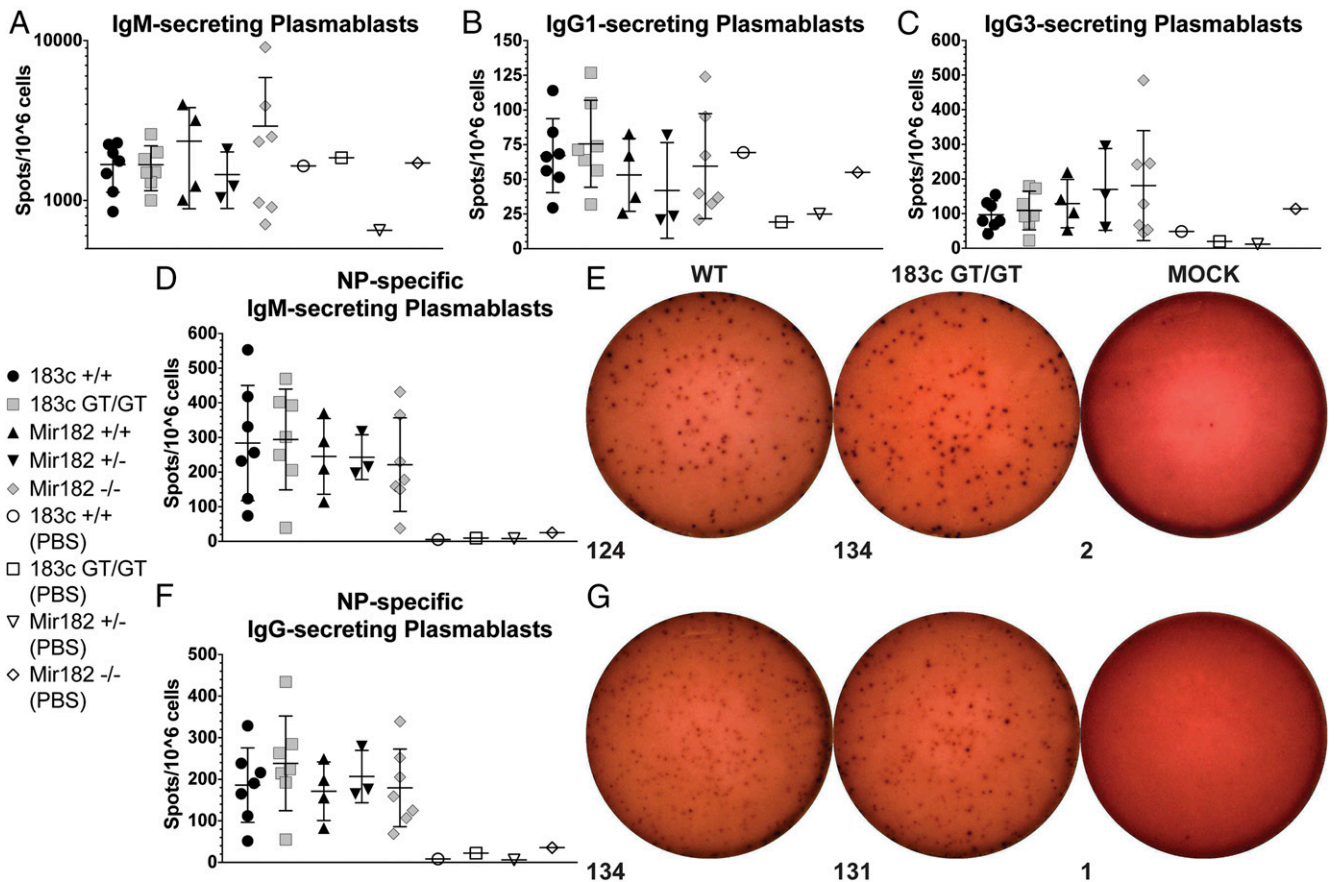
FIGURE 10. 183c miRNAs are not required for humoral response to TI-2 Ag NP-Ficoll. 183c$^{GT/GT}$, 183c$^{+/+}$, $Mir182^{-/-}$, $Mir182^{+/-}$, and $Mir182^{+/+}$ mice were i.p. immunized with 100 μg of NP(30)-AECM-Ficoll in sterile PBS and sacrificed on day 5. Total splenocytes were analyzed by ELISpot. Quantification of IgM- (**A**), IgG1- (**B**), and IgG3-secreting (**C**) plasmablasts per 10^6 cells. (**D** and **E**) NP-specific IgM-secreting plasmablast quantification per 10^6 cells (D) and representative membrane images of wells seeded with 0.5 × 10^6 cells (E). (**F** and **G**) NP-specific IgG-secreting plasmablast quantification per 10^6 cells (F) and representative membrane images of wells seeded with 0.5 × 10^6 cells (G). Numbers below images represent spot counts done in CTL ImmunoSpot software (E and G). $n = 7$ for 183c$^{GT/GT}$, 183c$^{+/+}$, and $Mir182^{-/-}$; $n = 4$ for $Mir182^{+/+}$; $n = 3$ for $Mir182^{+/-}$; $n = 1$ for mock immunization (PBS) controls; one experiment. Statistical significance was determined by ratio paired t test. All 183c$^{GT/GT}$ versus 183c$^{+/+}$, $Mir182^{-/-}$ versus $Mir182^{+/-}$, $Mir182^{-/-}$ versus $Mir182^{+/+}$, and $Mir182^{-/-}$ versus pooled $Mir182^{+/-}$/$Mir182^{+/+}$ comparisons failed to meet statistical significance ($\alpha = 0.05$).

It is thus reasonable to conclude that *FoxO1* is not a major 183c miRNA target in GC B cells.

Moreover, we present persuasive evidence that the absence of a phenotype in $Mir182^{-/-}$ B cells is not due to masking by clustered paralogs miR-183 and miR-96. The simplest interpretation is that 183c miRNA activity is unimportant for proximal humoral response processes. Perhaps the intense observed induction of 183c expression serves a role in a context that has not been studied or, alternatively, is purely vestigial in mammalian B cells. Another possibility is that there are other, yet to be described 183c miRNA paralogs in the mouse genome that compensate for 183c miRNA absence. Mining the TargetScan miRNA family database (32), we found evidence for just this scenario. For example, there is annotation for a miR-96 paralog, miR-1271, in the *Homo sapiens*, *Pan troglodytes* (chimpanzee), *Macaca mulatta* (rhesus macaque), *Bos taurus* (bovine), and *Canis familiaris* (canine) genomes (61), as well as a miR-183 paralog, miR-891b-3p, in the *M. mulatta* genome.

A final possibility is neatly illustrated by published reports in *Caenorhabditis elegans*. Systematic knockout of individual miRNAs, expected to unveil a bounty of developmental phenotypes, revealed startlingly few phenotypes (62, 63). In a fascinating follow-up, these individual mutants were reappraised in the context of a sensitized background. For example, miRNA activity was slashed by eliminating *alg-1*, one of two

Argonaute-like proteins in *C. elegans*. Strikingly, a wealth of phenotypes was uncovered (64). This suggests that the miRNA:target interaction network was robust enough to cope with individual perturbations, perhaps by rewiring in such a way as to fulfill the repressive activity that was lost. Speculatively, compensatory rewiring might entail miRNAs dissociating from weaker, perhaps less consequential, interactions to participate in stronger associations with functional binding sites that have become available upon loss of another miRNA (Fig. 11). This is possible, of course, within the confines of our current understanding of miRNA:target interaction (e.g., seed complementarity, conceivably by coopting bona fide unidentified paralogs and/or more distantly related miRNAs that retain sufficient similarity to overlap activity). Overlapping miRNA binding sites that are offset would necessitate even less homology among competing miRNAs to achieve layered repression. Decreasing overall miRNA levels nonspecifically would be expected to stifle this robustness, and this is precisely what was observed on the *alg-1* sensitized background. Intriguingly, *Ago2* (encoding Argonaute2) is a common predicted target of all three 183c miRNAs (Supplemental Table II), suggesting the tantalizing possibility of a protective feedback loop that enhances miRNA:target interaction network robustness upon the loss of 183c miRNA expression. However, we were unable to detect any difference in *Ago2* transcript levels between WT and 183c$^{GT/GT}$ GC B cells (Supplemental Fig. 1).
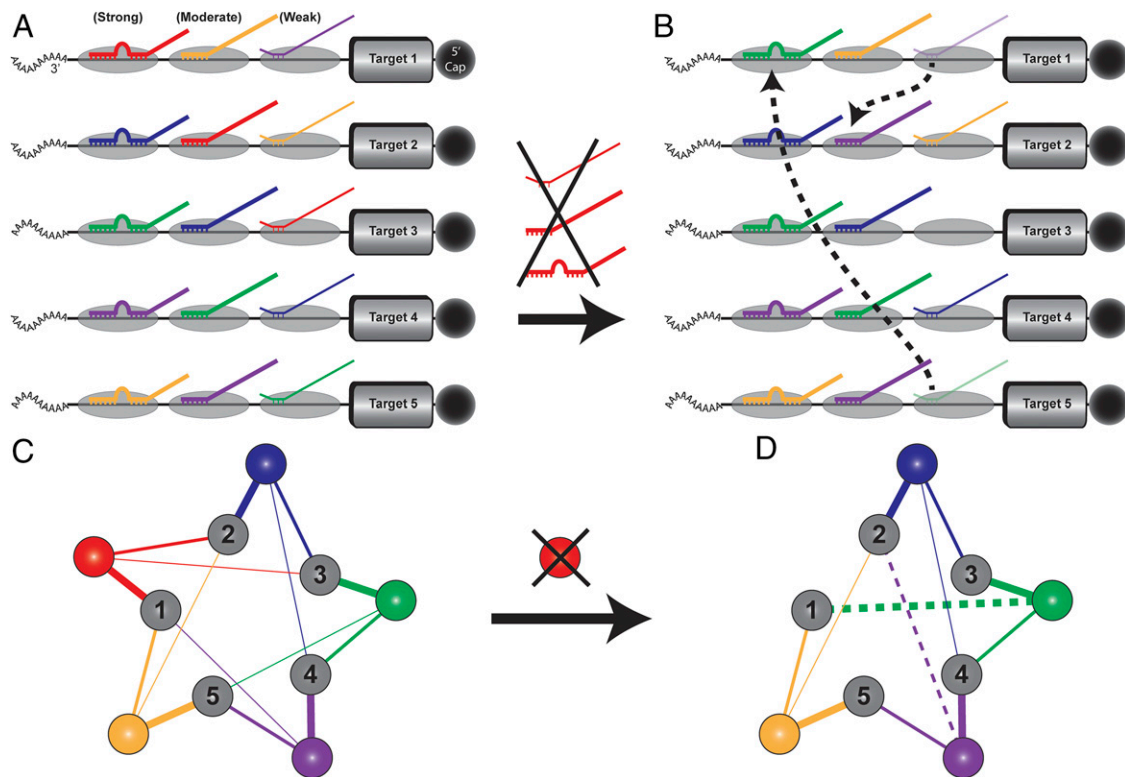
FIGURE 11. Schematic diagram of miRNA:target interaction network rewiring. (**A** and **B**) Depicted are five mRNA transcripts targeted in 3′ untranslated region miRNA binding sites (gray ellipses) by five different miRNA species distinguished by color. Gray boxes represent transcript open reading frames. Three levels of miRNA:target interaction strength, determined by extent of sequence complementarity, are shown as "Strong," "Moderate," and "Weak." In this simple model, target repression correlates with strength of interaction, and weak interactions confer little to no functional consequence. Each transcript participates in one miRNA interaction of each level. Upon ablation of the red miRNA species, green and purple miRNA weak interactions are abandoned in favor of stronger interactions that were previously outcompeted by red miRNA (B). The result is that weak interactions are sacrificed, but each target is still repressed by a strong and moderate interaction. (**C** and **D**) The same scenario is depicted using network diagrams. Numbered nodes represent targets 1–5, colored nodes represent the five miRNA species, and the thickness of edges signifies the strength of the interaction. Upon ablation of the red miRNA species, green and purple miRNA weak interactions are again abandoned in favor of stronger interactions that were previously outcompeted by red miRNA (D). New interactions are indicated by dotted lines.

Accordingly, greater emphasis on overall network activity in miRNA studies is an imperative implication of our work. Our results add to the growing body of evidence intimating an underappreciated miRNA:target interaction network robustness that compromises the utility of traditional genetic approaches in studying miRNAs and advocates an approach that considers the perspective of the entire network rather than only individual nodes.

Disclosures

The authors have no financial conflicts of interest.

References

1. Parra, D., F. Takizawa, and J. O. Sunyer. 2013. Evolution of B cell immunity. *Annu. Rev. Anim. Biosci.* 1: 65–97.
2. Suurmond, J., and B. Diamond. 2015. Autoantibodies in systemic autoimmune diseases: specificity and pathogenicity. *J. Clin. Invest.* 125: 2194–2202.
3. Lech, M., and H.-J. Anders. 2013. The pathogenesis of lupus nephritis. *J. Am. Soc. Nephrol.* 24: 1357–1366.
4. Mesin, L., J. Ersching, and G. D. Victora. 2016. Germinal center B cell dynamics. *Immunity* 45: 471–482.
5. Thorley-Lawson, D., K. W. Deitsch, K. A. Duca, and C. Torgbor. 2016. The link between *Plasmodium falciparum* malaria and endemic Burkitt's lymphoma-new insight into a 50-year-old enigma. *PLoS Pathog.* 12: e1005331.
6. Shalapour, S., and M. Karin. 2015. Immunity, inflammation, and cancer: an eternal fight between good and evil. *J. Clin. Invest.* 125: 3347–3355.
7. Keim, C., D. Kazadi, G. Rothschild, and U. Basu. 2013. Regulation of AID, the B-cell genome mutator. *Genes Dev.* 27: 1–17.
8. Vaidyanathan, B., W.-F. Yen, J. N. Pucella, and J. Chaudhuri. 2014. AIDing chromatin and transcription-coupled orchestration of immunoglobulin class-switch recombination. *Front. Immunol.* 5: 120.
9. Matthews, A. J., S. Zheng, L. J. DiMenna, and J. Chaudhuri. 2014. Regulation of immunoglobulin class-switch recombination: choreography of noncoding transcription, targeted DNA deamination, and long-range DNA repair. *Adv. Immunol.* 122: 1–57.
10. Rana, T. M. 2007. Illuminating the silence: understanding the structure and function of small RNAs. *Nat. Rev. Mol. Cell Biol.* 8: 23–36.
11. Bartel, D. P. 2009. MicroRNAs: target recognition and regulatory functions. *Cell* 136: 215–233.
12. Wienholds, E., and R. H. A. Plasterk. 2005. MicroRNA function in animal development. *FEBS Lett.* 579: 5911–5922.
13. Alvarez-Garcia, I., and E. A. Miska. 2005. MicroRNA functions in animal development and human disease. *Development* 132: 4653–4662.
14. Sun, K., and E. C. Lai. 2013. Adult-specific functions of animal microRNAs. *Nat. Rev. Genet.* 14: 535–548.
15. Xiao, C., and K. Rajewsky. 2009. MicroRNA control in the immune system: basic principles. *Cell* 136: 26–36.
16. Lawrie, C. H. 2013. MicroRNAs in hematological malignancies. *Blood Rev.* 27: 143–154.
17. Lin, S., and R. I. Gregory. 2015. MicroRNA biogenesis pathways in cancer. *Nat. Rev. Cancer* 15: 321–333.
18. Dambal, S., M. Shah, B. Mihelich, and L. Nonn. 2015. The microRNA-183 cluster: the family that plays together stays together. *Nucleic Acids Res.* 43: 7173–7188.

19. Flynt, A. S., and E. C. Lai. 2008. Biological principles of microRNA-mediated regulation: shared themes amid diversity. *Nat. Rev. Genet.* 9: 831–842.

20. Ebert, M. S., and P. A. Sharp. 2012. Roles for microRNAs in conferring robustness to biological processes. *Cell* 149: 515–524.

21. Moskwa, P., F. M. Buffa, Y. Pan, R. Panchakshari, P. Gottipati, R. J. Muschel, J. Beech, R. Kulshrestha, K. Abdelmohsen, D. M. Weinstock, et al. 2011. miR-182-mediated downregulation of BRCA1 impacts DNA repair and sensitivity to PARP inhibitors. [Published erratum appears in 2014 *Mol. Cell* 53: 162–163.] *Mol. Cell* 41: 210–220.

22. Krishnan, K., A. L. Steptoe, H. C. Martin, S. Wani, K. Nones, N. Waddell, M. Mariasegaram, P. T. Simpson, S. R. Lakhani, B. Gabrielli, et al. 2013. MicroRNA-182-5p targets a network of genes involved in DNA repair. *RNA* 19: 230–242.

23. Stittrich, A. B., C. Haftmann, E. Sgouroudis, A. A. Kühl, A. N. Hegazy, I. Panse, R. Riedel, M. Flossdorf, J. Dong, F. Fuhrmann, et al. 2010. The microRNA miR-182 is induced by IL-2 and promotes clonal expansion of activated helper T lymphocytes. *Nat. Immunol.* 11: 1057–1062.

24. Pucella, J. N., W.-F. Yen, M. V. Kim, J. van der Veeken, N. D. Socci, Y. Naito, M. O. Li, N. Iwai, and J. Chaudhuri. 2015. miR-182 is largely dispensable for adaptive immunity: lack of correlation between expression and function. [Published erratum appears in 2015 *J. Immunol.* 195: 1903.] *J. Immunol.* 194: 2635–2642.

25. Lumayag, S., C. E. Haldin, N. J. Corbett, K. J. Wahlin, C. Cowan, S. Turturro, P. E. Larsen, B. Kovacs, P. D. Witmer, D. Valle, et al. 2013. Inactivation of the microRNA-183/96/182 cluster results in syndromic retinal degeneration. *Proc. Natl. Acad. Sci. USA* 110: E507–E516.

26. Jin, Z. B., G. Hirokawa, L. Gui, R. Takahashi, F. Osakada, Y. Hiura, M. Takahashi, O. Yasuhara, and N. Iwai. 2009. Targeted deletion of miR-182, an abundant retinal microRNA. *Mol. Vis.* 15: 523–533.

27. Schmittgen, T. D., and K. J. Livak. 2008. Analyzing real-time PCR data by the comparative C(T) method. *Nat. Protoc.* 3: 1101–1108.

28. Li, Y.-F., X. Ou, S. Xu, Z.-B. Jin, N. Iwai, and K.-P. Lam. 2016. Loss of miR-182 affects B-cell extrafollicular antibody response. *Immunology* 148: 140–149.

29. Kelada, S., P. Sethupathy, I. S. Okoye, E. Kistasis, S. Czieso, S. D. White, D. Chou, C. Martens, S. M. Ricklefs, K. Virtaneva, et al. 2013. miR-182 and miR-10a are key regulators of Treg specialisation and stability during Schistosome and *Leishmania*-associated inflammation. *PLoS Pathog.* 9: e1003451.

30. Donatelli, S. S., J.-M. Zhou, D. L. Gilvary, E. A. Eksioglu, X. Chen, W. D. Cress, E. B. Haura, M. B. Schabath, D. Coppola, S. Wei, and J. Y. Djeu. 2014. TGF-β-inducible microRNA-183 silences tumor-associated natural killer cells. *Proc. Natl. Acad. Sci. USA* 111: 4203–4208.

31. Ichiyama, K., A. Gonzalez-Martin, B. S. Kim, H. Y. Jin, W. Jin, W. Xu, M. Sabouri-Ghomi, S. Xu, P. Zheng, C. Xiao, and C. Dong. 2016. The MicroRNA-183-96-182 cluster promotes T helper 17 cell pathogenicity by negatively regulating transcription factor Foxo1 expression. *Immunity* 44: 1284–1298.

32. Agarwal, V., G. W. Bell, J.-W. Nam, and D. P. Bartel. 2015. Predicting effective microRNA target sites in mammalian mRNAs. *Elife* 4: e05005.

33. Xu, S., P. D. Witmer, S. Lumayag, B. Kovacs, and D. Valle. 2007. MicroRNA (miRNA) transcriptome of mouse retina and identification of a sensory organ-specific miRNA cluster. *J. Biol. Chem.* 282: 25053–25066.

34. Victora, G. D., and M. C. Nussenzweig. 2012. Germinal centers. *Annu. Rev. Immunol.* 30: 429–457.

35. Kawai, T., and S. Akira. 2006. TLR signaling. *Cell Death Differ.* 13: 816–825.

36. Mackay, F., and P. Schneider. 2009. Cracking the BAFF code. *Nat. Rev. Immunol.* 9: 491–502.

37. Elgueta, R., M. J. Benson, V. C. de Vries, A. Wasiuk, Y. Guo, and R. J. Noelle. 2009. Molecular mechanism and function of CD40/CD40L engagement in the immune system. *Immunol. Rev.* 229: 152–172.

38. Shinall, S. M., M. Gonzalez-Fernandez, R. J. Noelle, and T. J. Waldschmidt. 2000. Identification of murine germinal center B cell subsets defined by the expression of surface isotypes and differentiation antigens. *J. Immunol.* 164: 5729–5738.

39. Klein, U., S. Casola, G. Cattoretti, Q. Shen, M. Lia, T. Mo, T. Ludwig, K. Rajewsky, and R. Dalla-Favera. 2006. Transcription factor IRF4 controls plasma cell differentiation and class-switch recombination. *Nat. Immunol.* 7: 773–782.

40. Paus, D., T. G. Phan, T. D. Chan, S. Gardam, A. Basten, and R. Brink. 2006. Antigen recognition strength regulates the choice between extrafollicular plasma cell and germinal center B cell differentiation. *J. Exp. Med.* 203: 1081–1091.

41. Crotty, S. 2014. T follicular helper cell differentiation, function, and roles in disease. *Immunity* 41: 529–542.

42. Jacob, J., R. Kassir, and G. Kelsoe. 1991. In situ studies of the primary immune response to (4-hydroxy-3-nitrophenyl)acetyl. I. The architecture and dynamics of responding cell populations. *J. Exp. Med.* 173: 1165–1175.

43. Kimoto, H., H. Nagaoka, Y. Adachi, T. Mizuochi, T. Azuma, T. Yagi, T. Sata, S. Yonehara, Y. Tsunetsugu-Yokota, M. Taniguchi, and T. Takemori. 1997. Accumulation of somatic hypermutation and antigen-driven selection in rapidly cycling surface Ig+ germinal center (GC) B cells which occupy GC at a high frequency during the primary anti-hapten response in mice. *Eur. J. Immunol.* 27: 268–279.

44. Jolly, C. J., N. Klix, and M. S. Neuberger. 1997. Rapid methods for the analysis of immunoglobulin gene hypermutation: application to transgenic and gene targeted mice. *Nucleic Acids Res.* 25: 1913–1919.

45. Sze, D. M., K. M. Toellner, C. García de Vinuesa, D. R. Taylor, and I. C. MacLennan. 2000. Intrinsic constraint on plasmablast growth and extrinsic limits of plasma cell survival. *J. Exp. Med.* 192: 813–821.

46. Weisel, F. J., G. V. Zuccarino-Catania, M. Chikina, and M. J. Shlomchik. 2016. A temporal switch in the germinal center determines differential output of memory B and plasma cells. *Immunity* 44: 116–130.

47. Nutt, S. L., P. D. Hodgkin, D. M. Tarlinton, and L. M. Corcoran. 2015. The generation of antibody-secreting plasma cells. *Nat. Rev. Immunol.* 15: 160–171.

48. Mond, J. J., A. Lees, and C. M. Snapper. 1995. T cell-independent antigens type 2. *Annu. Rev. Immunol.* 13: 655–692.

49. MacLennan, I. C. M., K.-M. Toellner, A. F. Cunningham, K. Serre, D. M.-Y. Sze, E. Zúñiga, M. C. Cook, and C. G. Vinuesa. 2003. Extrafollicular antibody responses. *Immunol. Rev.* 194: 8–18.

50. Vinuesa, C. G., and P. P. Chang. 2013. Innate B cell helpers reveal novel types of antibody responses. *Nat. Immunol.* 14: 119–126.

51. Barwick, B. G., C. D. Scharer, A. P. R. Bally, and J. M. Boss. 2016. Plasma cell differentiation is coupled to division-dependent DNA hypomethylation and gene regulation. *Nat. Immunol.* 17: 1216–1225.

52. García de Vinuesa, C., P. O'Leary, D. M. Sze, K. M. Toellner, and I. C. MacLennan. 1999. T-independent type 2 antigens induce B cell proliferation in multiple splenic sites, but exponential growth is confined to extrafollicular foci. *Eur. J. Immunol.* 29: 1314–1323.

53. Hsu, M.-C., K.-M. Toellner, C. G. Vinuesa, and I. C. M. Maclennan. 2006. B cell clones that sustain long-term plasmablast growth in T-independent extrafollicular antibody responses. *Proc. Natl. Acad. Sci. USA* 103: 5905–5910.

54. Schwickert, T. A., R. L. Lindquist, G. Shakhar, G. Livshits, D. Skokos, M. H. Kosco-Vilbois, M. L. Dustin, and M. C. Nussenzweig. 2007. In vivo imaging of germinal centres reveals a dynamic open structure. *Nature* 446: 83–87.

55. Hodgkin, P. D., J. H. Lee, and A. B. Lyons. 1996. B cell differentiation and isotype switching is related to division cycle number. *J. Exp. Med.* 184: 277–281.

56. Hasbold, J., A. B. Lyons, M. R. Kehry, and P. D. Hodgkin. 1998. Cell division number regulates IgG1 and IgE switching of B cells following stimulation by CD40 ligand and IL-4. *Eur. J. Immunol.* 28: 1040–1051.

57. He, M., E. M. Cortizas, R. E. Verdun, and E. Severinson. 2015. Cyclin-dependent kinases regulate Ig class switching by controlling access of AID to the switch region. *J. Immunol.* 194: 4231–4239.

58. Dominguez-Sola, D., J. Kung, A. B. Holmes, V. A. Wells, T. Mo, K. Basso, and R. Dalla-Favera. 2015. The FOXO1 transcription factor instructs the germinal center dark zone program. *Immunity* 43: 1064–1074.

59. Sander, S., V. T. Chu, T. Yasuda, A. Franklin, R. Graf, D. P. Calado, S. Li, K. Imami, M. Selbach, M. Di Virgilio, et al. 2015. PI3 Kinase and FOXO1 transcription factor activity differentially control B cells in the germinal center light and dark zones. *Immunity* 43: 1075–1086.

60. Zhang, D., Y. Li, X. Yao, H. Wang, L. Zhao, H. Jiang, X. Yao, S. Zhang, C. Ye, W. Liu, et al. 2016. miR-182 regulates metabolic homeostasis by modulating glucose utilization in muscle. *Cell Rep.* 16: 757–768.

61. Jensen, K. P., and J. Covault. 2011. Human miR-1271 is a miR-96 paralog with distinct non-conserved brain expression pattern. *Nucleic Acids Res.* 39: 701–711.

62. Miska, E. A., E. Alvarez-Saavedra, A. L. Abbott, N. C. Lau, A. B. Hellman, S. M. McGonagle, D. P. Bartel, V. R. Ambros, and H. R. Horvitz. 2007. Most *Caenorhabditis elegans* microRNAs are individually not essential for development or viability. *PLoS Genet.* 3: e215.

63. Alvarez-Saavedra, E., and H. R. Horvitz. 2010. Many families of C. elegans microRNAs are not essential for development or viability. *Curr. Biol.* 20: 367–373.

64. Brenner, J. L., K. L. Jasiewicz, A. F. Fahley, B. J. Kemp, and A. L. Abbott. 2010. Loss of individual microRNAs causes mutant phenotypes in sensitized genetic backgrounds in C. elegans. *Curr. Biol.* 20: 1321–1325.